**Table 1.** Clinical features of patients[a]

| Diagnosis | No. of cases | Age (years) | Sex (M/F) | Duration prior to biopsy (days) |
| --- | --- | --- | --- | --- |
| Microscopic polyangiitis | 5 | 64.8±17.5 (44–84) | 2/3 | 5.6 (2–8) |
| Non-systemic vasculitic neuropathy | 3 | 67.5±3.5 (64–71) | 2/1 | 7.3 (2–14) |
| Normal-appearing nerves | 5 | 63.2±5.6 (56–76) | 3/2 | – |

[a] Age is expressed as mean±S.D. (range). Duration prior to biopsy is expressed as mean (range). –, not applicable.

sults and discuss the role of NGF produced in different cell types.

# EXPERIMENTAL PROCEDURES

## Patients and sural nerve biopsies

Sural nerve specimens were obtained from diagnostic sural nerve biopsies from eight patients with vasculitic neuropathies (four women, four men; mean age, 66.6 years; age range, 44–84 years). The patients consisted of five patients with microscopic polyangiitis and three with non-systemic vasculitic neuropathy (Table 1). Patients underwent neurological assessment, cerebrospinal fluid analysis, cranial magnetic resonance imaging (MRI) computed tomography (CT), routine blood and urine studies, nerve conduction studies, sural nerve biopsies and therapeutic trials with corticosteroids. The diagnosis of the various categories of vasculitic neuropathy was based on the criteria adopted by the Chapel Hill Consensus Conference in 1994 (Jennette et al., 1994). Sural nerve biopsies were performed within 2 weeks (usually 1 week) after the onset of neuropathy prior to treatment (2–14 days, mean 6.5 days), and the samples were histologically examined as described previously (Hattori et al., 1999). Five sural nerve specimens with normal morphology were obtained from age-matched (56–76 years) individuals and served as controls. Informed consent was obtained from each patient. The study was approved by the ethics committee of Nagoya University Graduate School of Medicine.

## Pathologic study

Other portions of the nerve segments were processed to prepare glutaraldehyde-fixed, epoxy-resin embedded semithin sections and formalin-fixed, paraffin-embedded sections to assess the morphology of the nerve fibers and any invading cells. Specimens were fixed in 2% glutaraldehyde in 0.025 M cacodylate buffer at pH 7.4, and processed for semithin, ultrathin, or teased-fiber studies. The density of myelinated fibers was assessed directly from the Toluidine Blue-stained semithin transverse sections of sural nerves using a computer-assisted image analyzer (Luzex FS; Nikon, Tokyo, Japan) as described previously (Sobue et al., 1988, 1998; Hattori et al., 1999). Teased fibers were isolated from one portion of glutaraldehyde-fixed specimens, and the pathological condition of each isolated fiber was evaluated (Sobue et al., 1988, 1998; Hattori et al., 1999). Axonal histopathologic features analyzed include axonal loss, and axonal degeneration in the teased-fiber preparations. In the transverse sections, clusters of two or three small myelinated fibers surrounded by basal lamina were designated as axonal regenerating sprouts, as described previously (Hattori et al., 1999; Koike et al., 2001). The population of fibers manifesting active axonal degeneration or a normal appearance per square millimeter was assessed by calculating the incidence of such fibers multiplied by the total population of myelinated fibers per square millimeter as described previously (Yamamoto et al., 1998b).

## *In situ* hybridization, immunohistochemical study and quantitative analyses

One portion of the sural nerve specimens was immediately frozen in liquid nitrogen and stored at −80 °C until use. Ten-micrometer thick frozen sections of sural nerves were prepared for *in situ* hybridization and immunohistochemical staining. Frozen sections were treated with proteinase K, refixed in 4% paraformaldehyde, and processed for *in situ* hybridization and immunohistochemistry. For *in situ* hybridization, digoxigenin-labeled cRNA probes were generated from linearized plasmids for NGF using SP6 or T7 RNA polymerase (Roche Diagnostics, Basel, Switzerland). Sliced sural nerves were hybridized for 16 h at 40 °C with the probes in a solution (50% formamide, 10 mM Tris–HCl, pH 7.6, 1 mM EDTA, 0.6 M NaCl, 0.25% SDS, 0.1 mg/ml yeast tRNA, 10% dextran sulfate, and 1× Denhardt's solution), washed and detected immunologically with alkaline phosphatase- or FITC-conjugated anti-digoxigenin antibody. Immunohistochemistry was performed by the ABC method for rhodamine signals according to the manufacturer's protocol, using antibodies against the following cell-specific markers: S100 (Sigma) antibody for Schwann cells; CD68 (DAKO), MRP14 (Dianova) and MRP8 (Dianova) for macrophages; CD4 (DAKO), CD8 (DAKO), UCHL-I (DAKO) and CD3 (DAKO) for T-cells. The cell infiltrates immunoreactive for macrophage marker (CD68) and T cell marker (UCHL-1) were counted to assess the degree of inflammatory cell invasion in the epineurial and endoneurial areas of the nerve segments.

To assess the degree of NGF mRNA expression in the nerve segments, the signal intensity of NGF mRNA was quantified using a CCD image analyzer (Zeiss Axiovert S100TV) as previously described (Mitsuma et al., 1999; Yamamoto et al., 2001). Perivascular inflammatory lesions in the epineurium were identified as regions of infiltrating cells surrounding necrotizing vasculitic vessels, in most cases vessel walls (from intima to adventitia) of vasculitic vessels. Lesions in the endoneurium were also identified as regions of nerve fiber damage accompanied by infiltrating cells. Within these lesions, macrophages (CD68-positive cells), T cells (UCHL-1-positive cells), Schwann cells (S-100-positive cells), and antigen-specific cells with different profiles (MRP-14-, MRP-8-, CD3-, CD4-, and CD8-positive cells) were identified and assessed to determine the cellular profiles of active lesions in vasculitic neuropathy. The cells with cell-specific markers and NGF mRNA signals were assessed on the captured images of the desired magnification using a fluorescence microscope with a CCD image analyzer and image analyzing software (NIH image): approximately 300 MRP-14-positive cells, 200 MRP-8-positive cells, 100 CD3-positive positive cells, 100 CD4-positive positive cells, and 100 CD8-positive positive cells were observed per lesion of interest. The frequency of a specific lineage of cells (MRP14, MRP8, CD3, CD4, CD8 or S100) producing NGF mRNA was quantified as the percentage of cells with NGF mRNA signals among the total cells with the cell-specific marker. The signal intensity of cell-lineage-specific NGF mRNA was quantified by measuring cellular NGF mRNA signals with the cell-specific marker in the lesion of interest (100×100 μm), and expressed as NGF mRNA signals per square millimeter for each specific lineage of cells in the epineurium and endoneurium.
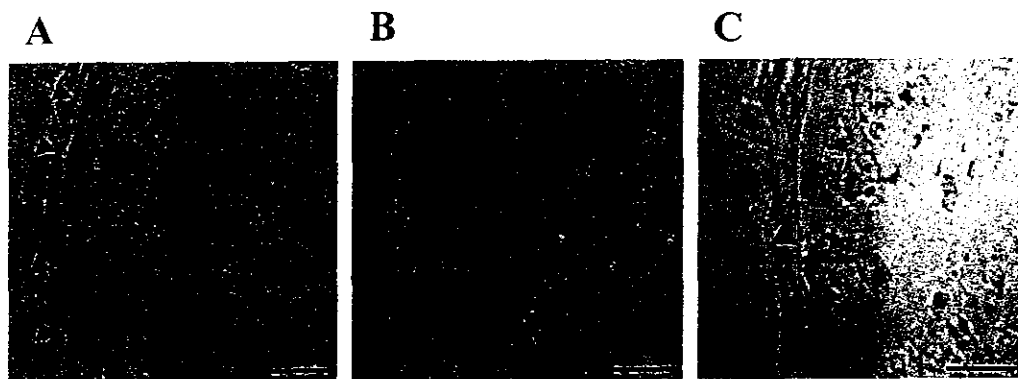
**Fig. 1.** *In situ* hybridization of NGF mRNA in vasculitic neuropathy.*In situ* hybridization with anti-sense (A and C) and sense probes (B) is shown. *In situ* hybridization of NGF mRNA indicated that NGF mRNA was expressed in the endoneurium and perineurium (arrows). Arrowhead indicates that perivascular cells expressed NGF mRNA. Scale bars=50 μm (A and B); 30 μm (C).

## Statistical analysis

For statistical analysis, the Mann-Whitney *U* test was used for comparison of *in situ* mRNA levels between pairs of individual groups. A simple correlation test was performed for correlation analysis.

## RESULTS

### NGF mRNA expression in a wide range of lineages of cells in nerve lesions

In vasculitic neuropathies, NGF mRNA signals were observed in the endoneurium and epineurium, where vessel wall cells were also positive for NGF mRNA (Fig. 1), whereas in control nerves only the endoneurial cells were slightly positive for NGF mRNA. NGF mRNA was also detected in the perineurial cells in vasculitic neuropathies (Fig. 1). Fluorescent double staining of NGF mRNA and cell-specific antigens revealed that NGF mRNA was highly expressed in macrophages, T cells and Schwann cells.

Macrophage marker staining showed that the expression level of NGF mRNA in round or oval shaped macrophages was higher than that in polymorphic macrophages (Fig. 2A–F). NGF mRNA levels in MRP14+ macrophages (Fig. 2G–I) were higher than those in MRP8+ cells (Fig. 2J–L). NGF mRNA expression levels, which were expressed as signal intensities per square millimeter and percentages of cells with NGF signals, were higher in MRP14+ macrophages compared with MRP8+ macrophages in the endoneurial lesions accompanying active axonal degeneration (Figs. 3A and 4A). NGF mRNA expression in MRP8+ macrophages was significantly greater in the epineurial space than in the endoneurial space, but that in MRP14+ macrophages did not differ between the epineurial and endoneurial spaces (Figs. 3A and 4A). Furthermore, overall NGF mRNA signal intensity, expressed as signal intensity per square millimeter, did not differ significantly between MRP8+ and MRP14+ macrophages in the epineurial lesions (Fig. 4A).

T cells with various cell surface markers expressed NGF mRNA (Fig. 2M–R). T cells expressed strong signals of NGF mRNA regardless of their surface markers, and almost all T cells produced NGF mRNA, especially in the

endoneurial space (Fig. 3 B). The proportions of epineurial CD4, CD8, or CD3 immunoreactive cells expressing NGF mRNA were slightly lower as compared with those of the corresponding endoneurial T cells (Fig. 3B). Since the proportions of T cell subtypes were similar in the endoneurial and epineurial lesions, the overall levels of NGF mRNA signals of each T cell subtype did not significantly differ from each other (Fig. 4B).

S100-immunopositive Schwann cells expressed NGF mRNA in the diseased nerves, whereas in control nerves NGF mRNA was expressed at a low level in Schwann cells (Figs. 2S–U, 3C and 4C). Even in the nerve lesions, the NGF mRNA signals of Schwann cells themselves were lower than those of the infiltrating cells, but the overall signal count was high due to the relatively higher Schwann cell population in neuropathic lesions (Fig. 4C). Moreover, NGF mRNA was also present in vessel wall cells in both the epineurium and endoneurium.

NGF mRNA was expressed in macrophages and T cells in perivascular lesions of the epineurial space, while in the endoneurium, Schwann cells, in addition to invading cells, synthesized NGF mRNA. The overall intensity of NGF mRNA levels per area in the endoneurium was high in Schwann cells and MRP14+ macrophages compared with other cell types, including T cells (Fig. 4). On the other hand, MRP14+ and MRP8+ macrophages were major cell types expressing NGF mRNA in the epineurial lesions.

### NGF mRNA expression and nerve regeneration

Pathological findings in the sural nerves of individual patients who had various vasculitic neuropathies and displayed the different NGF mRNA expression patterns are shown in Table 2. The pathological findings were highly variable among the patients, and independent of the underlying diseases causing vasculitic neuropathies. Axonal degeneration characteristic of vasculitic neuropathies was seen in all the patients, and axonal sprouts of regeneration were also associated with axonal pathology. The patients with more axonal sprouts demonstrated higher NGF mRNA levels not only in the endoneurium but also in the epineurium, as compared with those with fewer axonal sprouts (Fig. 5A and B). The endoneurial NGF mRNA
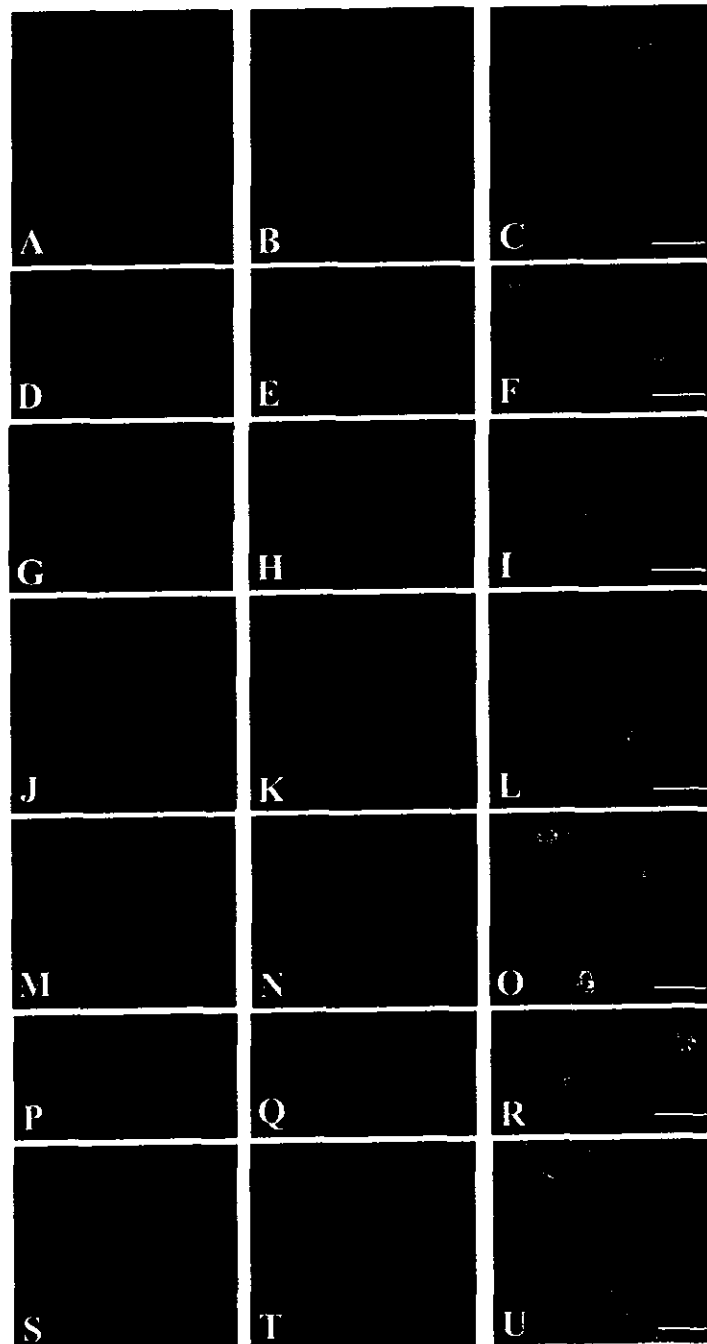
**Fig. 2.** Representative double staining of NGF mRNA in cells with various cell-specific markers. Double staining (merged yellow) of cells with various cell-specific markers (red) and NGF mRNA (green) is shown. NGF mRNA was strongly expressed in round and MRP14+ macrophages. T cells expressed strong signals of NGF mRNA. NGF mRNA signals in Schwann cells were weaker than those in the infiltrating cells. (A–C) Epineurial CD68+ cells; (D–F) endoneurial CD68+ cells; (G–I) endoneurial MRP14+ cell; (J–L) endoneurial MRP8+ cell; (M–O) epineurial UCHL-1+ cells; (P–R) endoneurial CD8+ cells; (S–U) S100+ cells. Scale bars=15 μm (A–F); 5 μm (G–L); 10 μm (M–R); 30 μm (S–U).

expression was more significantly correlated with axonal regenerating sprouts than epineurial one ($r$=0.84, $P$<0.01 vs. $r$=0.52, $P$=0.18). Furthermore, *in situ* Schwann cell NGF mRNA levels were correlated with the extent of axonal sprouts ($r$=0.75, $P$<0.05, Fig. 5C). The degree of NGF mRNA expression was well correlated with the extent of active axonal sprouting, but not with that of axonal

degeneration, independent of the distribution of NGF mRNA expression.

## DISCUSSION

NGF is known to support mainly small-diameter sensory neurons in DRG, and to express tropic activity for small

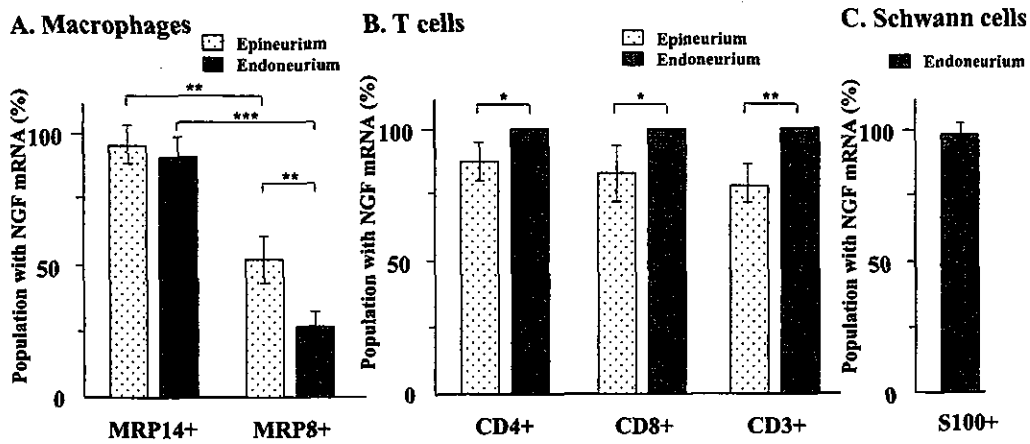**A. Macrophages**     **B. T cells**     **C. Schwann cells**



Fig. 3. Cell populations with NGF mRNA in the epineurial and endoneurial spaces. The cell populations with NGF mRNA signals and cell-specific markers were quantified as described in the text, and were expressed as percentages of cells with NGF mRNA signals in the epineurium and endoneurium in each patient. Mean±S.E. from the eight patients is indicated. * $P<0.05$, ** $P<0.01$, *** $P<0.001$.

myelinated and unmyelinated fibers of sensory nerves even in the adults (Rich et al., 1984; Unger et al., 1998). The high-affinity receptor TrkA for NGF is expressed in these neurons and their axons, but Schwann cells associated with small myelinated and unmyelinated fibers do not express TrkA. We demonstrated here for the first time the histological localization of NGF mRNA expression in the nerves of human neuropathy, using double staining with FITC and rhodamine to detect NGF mRNA and cell-specific antigens, respectively. NGF mRNA was expressed in the infiltrating macrophages and T cells, Schwann cells and perivascular cells in the nerve lesions. Expression of NGF mRNA in the infiltrating cells and other cells varied depending on the histological profiles and cell types. We have previously reported that in vasculitic neuropathies, the expression of NGF mRNA changed to a variable extent, and the mean levels of NGF mRNA were markedly increased compared with those of controls (Yamamoto et al., 2001). We also showed previously by a multiple regression analysis that NGF mRNA expression in

the nerve lesions was closely related to the invasion of macrophages and T cells (Yamamoto et al., 2001). Our previous study using whole nerve homogenates, however, failed to determine which specific lineages of cells express NGF mRNA to what extent, and how cell-type-specific NGF expression is correlated with axonal pathology.

Macrophage recruitment is an important component of NGF synthesis and of sensory axon maintenance and re-growth (Brown et al., 1991; Luk et al., 2003). Endoneurial infiltration by macrophages is observed in Wallerian degeneration as well as in autoimmune polyneuropathies, which show phenotypic and functional heterogeneity of macrophages with respect to morphology, specific marker antigens and residency (Kiefer et al., 1998). The expression of NGF mRNA was higher in oval or round-shaped macrophages than in macrophages with an irregular or ramified appearance. Round-shaped macrophages are reported to be activated for secretion of humoral immune factors such as cytokines, whereas irregular-shaped mac-

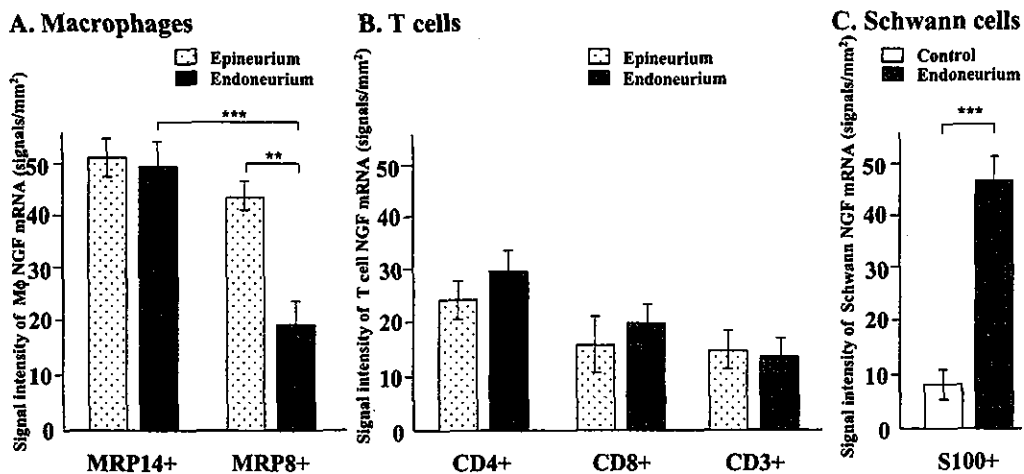**A. Macrophages**     **B. T cells**     **C. Schwann cells**



Fig. 4. Signal intensity of NGF mRNA in the epineurial and endoneurial macrophages, T cells and Schwann cells. The intensity of NGF mRNA signals with specific cell-specific markers was quantified as described in the text, and was expressed as signal intensity per square millimeter in the epineurium and endoneurium in each patient. Mean±S.E. from the eight patients and five controls is indicated. The white bar in C denotes Schwann cell expression of NGF mRNA in control nerves. * $P<0.05$, ** $P<0.01$, *** $P<0.001$.

Table 2. Pathological findings of sural nerve biopsies in the patients with vasculitic neuropathies[a]

| Case | Age (years)/Sex | Diagnosis | MF density (No./mm$^2$) | Axonal degeneration (%) | Active axonal degeneration (No./mm$^2$) | Axonal regeneration: sprouts (No./mm$^2$) | Infiltrates in epineurium Mφ/T cells (No./mm$^2$) | Infiltrates in endoneurium Mφ/T cells (No./mm$^2$) |
|------|-----------------|-----------|-------------------------|-------------------------|------------------------------------------|---------------------------------------------|----------------------------------------------------|----------------------------------------------------|
| 1 | 44/M | MP | 2884 | 14 | 404 | 193 | 228/28 | 213/24 |
| 2 | 84/F | MP | 909 | 95 | 864 | 59 | 352/19 | 323/38 |
| 3 | 66/F | MP | 3081 | 9 | 277 | 262 | 449/38 | 407/25 |
| 4 | 51/F | MP | 303 | 93 | 282 | 53 | 511/51 | 272/15 |
| 5 | 79/M | MP | 1264 | 98 | 1239 | 93 | 288/20 | 148/8 |
| 6 | 71/M | Non-systemic | 7467 | 4 | 299 | 15 | 215/12 | 181/9 |
| 7 | 74/F | Non-systemic | 6557 | 33 | 2163 | 30 | 318/18 | 151/9 |
| 8 | 64/M | Non-systemic | 3318 | 93 | 3086 | 10 | 189/15 | 88/11 |

[a] Active axonal degeneration, axonal degeneration×MF density; MF, myelinated fiber; MP, microscopic polyangitis.
The immunoreactive cell infiltrates for macrophage marker (CD68) and T cell marker (UCHL-1) were counted to assess the degree of inflammatory cell invasion in the epineurial and endoneurial areas of the nerve segments.

rophages act as scavengers of tissue degradation products and myelin debris (Marcinkiewicz et al., 1999). Macrophages bearing MRP14, a macrophage differentiation antigen associated with early active lesions (Kiefer et al., 1998), expressed more NGF mRNA in both the epineurial and endoneurial spaces of the lesioned nerves. Most of MRP14+ macrophages were round-shaped. In contrast, macrophages expressing MRP8, a macrophage differentiation antigen in chronic lesions (Kiefer et al., 1998) expressed less NGF mRNA, especially in the endoneurium. These findings suggest that NGF expressed in round-shaped and MRP14+ macrophages can be an early signal for the regeneration and repair process in vasculitic nerve lesions. NGF expression by macrophages in the endoneurium has been reported to be up-regulated by inflammatory reactions where cytokines such as IL-1β are expressed, and to lead to the establishment of a favorable environment for nerve repair and recovery (Deprez et al., 2001; Shamash et al., 2002). NGF-negative or weakly positive macrophages, most of which are MRP8+ and irregular-shaped, are thought to function in phagocytosis of myelin debris in the endoneurium, also promoting nerve regeneration (Marcinkiewicz et al., 1999). Moreover,

epineurial MRP8+ macrophages harbor relatively higher levels of NGF mRNA compared with endoneurial cells, and may collaborate with T cells in an immunoregulatory cascade of vasculitic neuropathy. Epineurial NGF from MRP14+ and MRP8+ macrophages may play an instrumental role in the perivascular inflammatory circuit, or alternatively may direct the repair of injured axons through the damaged permeable perineurium (Sugimoto et al., 2002).

In addition to macrophages, infiltrating T cells also expressed NGF mRNA, regardless of whether their surface markers identified them as helper CD4+, suppressor CD8+, or activating CD3+. The expression pattern of NGF mRNA in T cells was different from that in macrophages: in macrophages, the level of NGF mRNA was heterogeneous depending on the cell shape and surface markers, but T cells in the endoneurium expressed NGF mRNA regardless of the T cell markers. It has been demonstrated previously that activated T cells produce NGF in lesions of the injured CNS or PNS to enhance nerve repair (Santambrogio et al., 1994; Moalem et al., 2000). The present study showed that T cells infiltrating the endoneurial space appear to be authorized to express NGF in. NGF
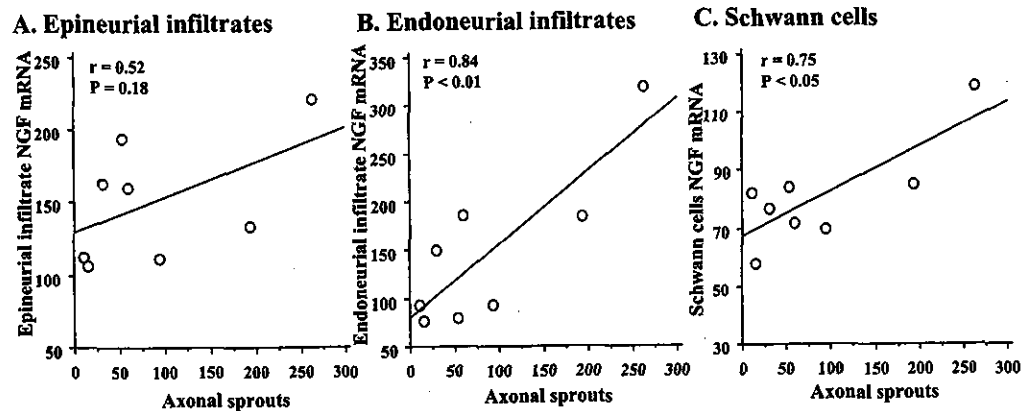
## A. Epineurial infiltrates    B. Endoneurial infiltrates    C. Schwann cells



**Fig. 5.** Relationship between nerve regeneration and NGF mRNA expression in the epineurial and endoneurial spaces. The intensity of NGF mRNA signals was quantified as described in the text, and was expressed as signal intensity per square millimeter for the epineurial and endoneurial infiltrates and Schwann cells in each patient. Simple correlation analysis was performed between regional NGF mRNA expression and axonal regenerating sprouts.

expressed in T cells in the epineurial perivascular lesions plays a secondary role to generate inflammation that may then function to bias toward a Th2 environment, which helps the interstitial reaction and subsequent recovery from a pathological condition (Santambrogio et al., 1994). T cells are obviously involved in the complex mechanism of formation and recovery of inflammatory pathology. NGF itself reportedly promotes differentiation of T cells (Matsuda et al., 1988; Ehrhard et al., 1993). NGF mRNA expression in CD4+ and CD8+ cells in the epineurial and endoneurial spaces may suggest that such up-regulation of NGF mRNA is one aspect of the complex network of events constituting nerve regeneration and repair.

Schwann cells are another NGF producer, as shown in the present study. NGF mRNA expression in Schwann cells was up-regulated and occurred diffusely in the endoneurium of the vasculitic lesions, suggesting that lesion-induced expression of NGF occurs in Schwann cells. In the endoneurium of the lesioned nerves, NGF is produced abundantly by Schwann cells as well as MRP14+ macrophages, and acts as a neurotrophic signal to promote axonal regeneration with TrkA in sensory axons. This putative cascade was supported by the present finding that NGF mRNA expression in Schwann cells was closely correlated with the degree of axonal regeneration sprouts.

Nerve injury by axotomy, in which axonal pathology with Wallerian degeneration is the major pathological process, is considered to be an analogous animal model of the endoneurial lesions in acute vasculitic neuropathies in human (Ito et al., 1998). In the axotomy model, IL-1β and IL-6 mRNAs rapidly increase after nerve damage, while NGF mRNA shows a two-peaked increase in the early and late phases (Ito et al., 1998). The early and late peaks of NGF mRNA expression are thought to occur in round-shaped epineurial hematogenous macrophages and Schwann cells, respectively. In human acute necrotizing vasculitic neuropathies in the present study, the nerve tissues were mostly obtained within 1 week after the onset of neuropathy. Pathological findings in the endoneurial space seem to correspond to the late phase of axotomized nerves in animals. This notion agrees with the findings that endoneurial NGF mRNA was mainly derived from Schwann cells as well as MRP14+ macrophages. As demonstrated here, MRP14+ early macrophages were also present concomitantly with MRP8+ late macrophages in the endoneurium of biopsied specimens. In addition to Schwann cells and macrophages, endoneurial fibroblasts may be another cellular source of NGF in the endoneurium of injured nerves as reported previously (Marcinkiewicz et al., 1999), since NGF mRNA signals was not completely consistent with the cellular markers for Schwann cells and macrophages.

We demonstrated that NGF mRNA expression in the infiltrating cells and Schwann cells showed a good correlation with the extent of axonal sprouts of regeneration but not with that of axonal degeneration. This finding is well consistent with our previous finding using multivariate analysis that NGF mRNA levels were not related to the extent of axonal degeneration (Yamamoto et al., 2001;

Sobue et al., 1998). NGF is known to induce axonal collateral sprouting in cell culture (Gallo and Letourneau, 1998; Itoh et al., 1998). Axonal regeneration is likely associated with NGF mRNA expression in the endoneurium mainly derived from MRP14+ macrophages as well as Schwann cells, and both types of cells collaborate in denervated nerves (Tofaris et al., 2002). The extent of axonal regeneration was very slight in the acute phase of vasculitic neuropathies, particularly as compared with the extent in chronic axonal neuropathy such as Charcot-Marie-Tooth disease type X (Hattori et al., 2003), showing abundant axonal sprouts. Direct evidence that activated macrophages are present at the sprouting sites was not found in this study, since the lesions caused by human vasculitic neuropathies are temporally and spatially multifocal and dispersive, not synchronous (Batchelor et al., 2002). As a correlation between the degree of axonal regeneration and the number of infiltrated macrophages is not significant in the present data, it is likely that NGF itself enhances axonal regeneration in nerve lesions of vasculitic neuropathies. Moreover, other neurotrophic factors such as brain-derived neurotrophic factor and neurotrophin-3 may be involved in axonal regeneration, since their mRNA expression levels were correlated with the extent of macrophage invasion in injured human nerves as reported in our previous studies (Sobue et al., 1998; Yamamoto et al., 1998b; Ito et al., 2001). Further studies whether axonal regenerating sprouts are the neuritis of peptidergic DRG neurons with TrkA will be needed.

Taken together, our findings on the double labeling of NGF mRNA and cellular markers clearly demonstrated that early-activated macrophages and Schwann cells are the major source of NGF expression in human nerve lesions of acute necrotizing vasculitic neuropathies, providing a clue about axonal regeneration and nerve repair. Targeted modulation of hematogenous macrophage NGF will help to promote nerve regeneration for the treatment of acute vasculitic neuropathies (Heuss et al., 2000). Further investigations will be required to determine how macrophage NGF, with the cytokine network, operates differentially in the epineurial and endoneurial areas for the recovery of vasculitic neuropathies.

## REFERENCES

Apfel SC, Arezzo JC, Lipson L, Kessler JA (1992) Nerve growth factor prevents experimental cisplatin neuropathy. Ann Neurol 31:76–80.

Batchelor PE, Porritt MJ, Martinello P, Parish CL, Liberatore GT, Donnan GA, Howells DW (2002) Macrophages and microglia produce local trophic gradients that stimulate axonal sprouting toward but not beyond the wound edge. Mol Cell Neurosci 21:436–453.

Brown MC, Perry VH, Lunn ER, Gordon S, Heumann R (1991) Macrophage dependence of peripheral sensory nerve regeneration: possible involvement of nerve growth factor. Neuron 6:359–370.

Chao MV, Hempstead BL (1995) p75 And Trk: a two-receptor system. Trends Neurosci 18:321–326.

Cosgaya JM, Chan JR, Shooter EM (2002) The neurotrophin receptor p75NTR as a positive modulator of myelination. Science 298:1245–1248.

Deprez M, Lubke U, Verlaet M, Debrus S, Delvenne P, Martin JJ (2001) Detection of cytokines in human sural nerve biopsies: an immunohistochemical and molecular study. Acta Neuropathol (Berl) 101:393–404.

Ehrhard PB, Erb P, Graumann U, Otten U (1993) Expression of nerve growth factor and nerve growth factor receptor tyrosine kinase Trk in activated CD4-positive T-cell clones. Proc Natl Acad Sci USA 90:10984–10988.

Fischer SJ, Podratz JL, Windebank AJ (2001) Nerve growth factor rescue of cisplatin neurotoxicity is mediated through the high affinity receptor: studies in PC12 cells and p75 null mouse dorsal root ganglia. Neurosci Lett 308:1–4.

Gallo G, Letourneau PC (1998) Localized sources of neurotrophins initiate axon collateral sprouting. J Neurosci 18:5403–5414.

Greeson DM, Moix L, Meier M, Armstrong DM, Wiley RG (1992) A continuing signal maintains NGF receptor expression in hypoglossal motor neurons after crush injury. Brain Res 594:351–355.

Hantzopoulous PA, Suri C, Glass DG (1994) The low affinity NGF receptor, p75, can collaborate with each of the Trks to potentiate functional responses to the neurotrophins. Neuron 13:187–201.

Hattori N, Ichimura M, Nagamatsu N, Li M, Yamamoto K, Kumazawa K, Mitsuma T, Sobue G (1999) Clinicopathological features of Churg-Strauss syndrome-associated neuropathy. Brain 122:427–439.

Hattori N, Yamamoto M, Yoshihara T, Koike H, Nakagawa M, Yoshikawa H, Ohnishi A, Hayasaka K, Onodera O, Baba M, Yasuda H, Saito T, Nakashima K, Kira J, Kaji R, Oka N, Sobue G (2003) Demyelinating and axonal features of Charcot-Marie-Tooth disease with mutations of myelin-related proteins (PMP22, MPZ and Cx32): a clinicopathological study of 205 Japanese patients. Brain 126:134–151.

Hawke SH, Davies LRP, Guo YP, Pollard JD, McLeod JG (1991) Vasculitic neuropathy: a clinical and pathological study. Brain 114:2175–2190.

Hayakawa K, Itoh T, Niwa H, Mutoh T, Sobue G (1998) NGF prevention of neurotoxicity induced by cisplatin, vincristine and taxol depends on toxicity of each drug and NGF treatment schedule: in vitro study of adult rat sympathetic ganglion explants. Brain Res 794:313–319.

Heumann R, Lindholm D, Bandtlow C, Meyer M, Radeke MJ, Misko TP, Shooter E, Thoenen H (1987) Differential regulation of mRNA encoding nerve growth factor and its receptor in rat sciatic nerve during development, degeneration, and regeneration: role of macrophages. Proc Natl Acad Sci USA 84:8735–8739.

Heuss D, Probst-Cousin S, Kayser C, Neundorfer B (2000) Cell death in vasculitic neuropathy. Muscle Nerve 23:999–1004.

Ito Y, Yamamoto M, Li M, Doyu M, Tanaka F, Mutoh T, Mitsuma T, Sobue G (1998) Differential temporal expression of mRNAs for ciliary neurotrophic factor (CNTF), leukemia inhibitory factor (LIF), interleukin-6 (IL-6), and their receptors (CNTFRα, LIFRβ, IL-6Rα and gp130) in injured peripheral nerves. Brain Res 793:321–327.

Ito Y, Yamamoto M, Mitsuma T, Li M, Hattori N, Sobue G (2001) Expression of mRNAs for ciliary neurotrophic factor (CNTF), leukemia inhibitory factor (LIF), interleukin-6 (IL-6), and their receptors (CNTFRα, LIFRβ, IL-6Rα and gp130) in human peripheral neuropathies. Neurochem Res 26:51–58.

Itoh T, Niwa H, Nagamatsu M, Mitsuma T, Miyakawa A, Pleasure D, Sobue G (1998) Nerve growth factor maintains regulation of intracellular calcium in neonatal sympathetic neurons but not in mature or aged neurons. Neuroscience 82:641–651.

Jennette JC, Falk RJ, Andrassy K (1994) Nomenclature of systemic vasculitides: proposal of an international consensus conference. Arthr Rheumat 37:187–192.

Kiefer R, Kieseier BC, Bruck W, Hartung HP, Toyka KV (1998) Macrophage differentiation antigens in acute and chronic autoimmune polyneuropathies. Brain 121:469–479.

Koike H, Mori K, Misu K, Hattori N, Ito H, Hirayama M, Sobue G (2001) Painful alcoholic polyneuropathy with predominant small-fiber loss and normal thiamine status. Neurology 56:1727–1732.

Levi-Montalcini R, Skaper SD, Dal Toso R, Petrelli L, Leon A (1996) Nerve growth factor: from neurotrophin to neurokine. Trends Neurosci 19:514–520.

Luk HW, Noble LJ, Werb Z (2003) Macrophages contribute to the maintenance of stable regenerating neurites following peripheral nerve injury. J Neurosci Res 73:644–658.

Marcinkiewicz M, Marcinkiewicz J, Chen A, Leclaire F, Chretien M, Richardson P (1999) Nerve growth factor and proprotein convertases furin and PC7 in transected sciatic nerves and in nerve segments cultured in conditioned media: their presence in Schwann cells, macrophages, and smooth muscle cells. J Comp Neurol 403:471–485.

Matsuda H, Coughlin MD, Bienenstock J, Denburg JA (1988) Nerve growth factor promotes human hemopoietic colony growth and differentiation. Proc Natl Acad Sci USA 85:6508–6512.

Mitsuma N, Yamamoto M, Li M, Ito Y, Mitsuma T, Mutoh T, Takahashi M, Sobue G (1999) Expression of GDNF receptor (RET and GD-NFR-α) mRNAs in the spinal cord of patients with amyotrophic lateral sclerosis. Brain Res 820:77–85.

Miyata Y, Kashihara Y, Homma S, Kuno M (1986) Effects of nerve growth factor on the survival and synaptic function of Ia sensory neurons axotomized in neonatal rats. J Neurosci 6:2012–2018.

Moalem G, Gdalyahu A, Shani Y, Otten U, Lazarovici P, Cohen IR, Schwartz M (2000) Production of neurotrophins by activated T cells: implications for neuroprotective autoimmunity. J Autoimmun 15:331–345.

Molliver DC, Wright DE, Leitner ML, Parsadanian AS, Doster K, Wen D, Yan Q, Snider WD (1997) IB4-binding DRG neurons switch from NGF to GDNF dependence in early postnatal life. Neuron 19:849–861.

Rich KM, Yip HK, Osborne PA, Schmidt RE, Johnson EM Jr (1984) Role of nerve growth factor in the adult dorsal root ganglia neuron and its response to injury. J Comp Neurol 230:110–118.

Rich KM, Luszczynski JR, Osborne PA (1987) Nerve growth factor protects adult sensory neurons from cell death and atrophy caused by nerve injury. J Neurocytol 16:261–268.

Santambrogio L, Benedetti M, Chao MV, Muzaffar R, Kulig K, Gabellini N, Hochwald G (1994) Nerve growth factor production by lymphocytes. J Immunol 153:4488–4495.

Shamash S, Reichert F, Rotshenker S (2002) The cytokine network of Wallerian degeneration: tumor necrosis factor- alpha, interleukin-1alpha, and interleukin-1beta. J Neurosci 22:3052–3060.

Snider WD, Wright DE (1996) Neurotrophins cause a new sensation. Neuron 16:229–232.

Sobue G, Yasuda T, Mitsuma T, Ross AH, Pleasure D (1988) Expression of nerve growth factor receptor in human peripheral neuropathies. Ann Neurol 24:64–72.

Sobue G, Yamamoto M, Doyu M, Li M, Yasuda T, Mitsuma T (1998) Expression of mRNAs for neurotrophic factor (NGF, BDNF and NT-3) and their receptors (p75NGFR, trkA, trkB and trkC) in human peripheral neuropathies. Neurochem Res 23:821–829.

Sugimoto Y, Takayama S, Horiuchi Y, Toyama Y (2002) An experimental study on the perineurial window. J Periph Nerv Syst 7:104–111.

Tofaris G, Patternson P, Jessen K, Mirsky R (2002) Denervated Schwann cells attract macrophages by secretion of leukemia inhibitory factor (LIF) and monocyte chemoattractant protein-1 in a process regulated by interleukin-6 and LIF. J Neurosci 22:6696–6703.

Unger JW, Klitzsch T, Pera S, Reiter R (1998) Nerve growth factor (NGF) and diabetic neuropathy in the rat: morphological investiga-

tions of the sural nerve, dorsal root ganglion, and spinal cord. Exp Neurol 153:23–34.

Yamamoto M, Li M, Nagamatsu M, Itoh T, Mutoh T, Mitsuma T, Sobue G (1998a) Expression of low-affinity neurotrophin receptor p75$^{NTR}$ in the peripheral nervous system of human neuropathies. Acta Neuropathol (Berl) 95:597–604.

Yamamoto M, Mitsuma N, Ito Y, Hattori N, Nagamatsu M, Li M,

Mitsuma T, Sobue G (1998b) Expression of GDNF and GDNFR-α mRNAs in human peripheral neuropathies. Brain Res 809:175–180.

Yamamoto M, Ito Y, Mitsuma N, Li M, Hattori N, Sobue G (2001) Pathology-related differential expression regulation of NGF, GDNF, CNTF, and IL-6 mRNAs in human vasculitic neuropathy. Muscle Nerve 24:830–833.

# Sodium butyrate ameliorates phenotypic expression in a transgenic mouse model of spinal and bulbar muscular atrophy

Makoto Minamiyama, Masahisa Katsuno, Hiroaki Adachi, Masahiro Waza, Chen Sang, Yasushi Kobayashi, Fumiaki Tanaka, Manabu Doyu, Akira Inukai and Gen Sobue*

Department of Neurology, Nagoya University Graduate School of Medicine, Nagoya 466-8550, Japan

Spinal and bulbar muscular atrophy (SBMA) is an inherited motor neuron disease caused by the expansion of a polyglutamine (polyQ) tract within the androgen receptor. Unifying mechanisms have been implicated in the pathogenesis of polyQ-dependent neurodegenerative diseases including SBMA, Huntington disease and spinocerebellar ataxias. It has been suggested that mutant protein containing polyQ inhibits histone acetyltransferase activity, resulting in transcriptional dysfunction and subsequent neuronal dysfunction. Histone deacetylase (HDAC) inhibitors alleviate neurological phenotypes in fly and mouse models of polyQ disease, although the therapeutic effect is limited by the toxicity of these compounds. We studied the therapeutic effects of sodium butyrate (SB), an HDAC inhibitor, in a transgenic mouse model of SBMA. Oral administration of SB ameliorated neurological phenotypes as well as increased acetylation of nuclear histone in neural tissues. These therapeutic effects, however, were seen only within a narrow range of SB dosage. Our results indicate that SB is a possible therapeutic agent for SBMA and other polyQ diseases, although an appropriate dose should be determined for clinical application.

## INTRODUCTION

Polyglutamine (polyQ) diseases are inherited neurodegenerative disorders caused by the expansion of a trinucleotide CAG repeat in the causative genes (1,2). To date, nine polyQ diseases have been identified (3). Spinal and bulbar muscular atrophy (SBMA) is a polyQ disease affecting males, and is characterized by proximal muscle atrophy, weakness, contraction fasciculations and bulbar involvement (4–6). The number of CAG repeats in the first exon of *androgen receptor* (*AR*) gene is polymorphic with a range of 11–35 in normal population; the repeat expands to 40–62 CAGs in SBMA patients (7,8) with minimal somatic mosaicism (9). There is an inverse correlation between the CAG repeat size in *AR* and the age at onset, or the disease severity (10–12) as observed in other polyQ diseases (1). The major pathological finding of SBMA is motor neuron loss in the spinal cord and brainstem accompanied by a subclinical loss of sensory neurons in the dorsal root ganglia (5). Nuclear inclusions (NIs) containing mutant AR have been observed in the residual motor neurons and non-neuronal cells (13,14). The presence of NIs, which is

a clue to the pathogenesis, is also striking in other polyQ diseases (15). These observations pointed to the cell nucleus as a crucial site of polyQ toxicity in the majority of polyQ diseases, although the exact role of NIs in the pathogenesis is yet to be elucidated (16). Our previous studies with a transgenic (Tg) mouse model of SBMA clearly demonstrated that reduction in the amount of nuclear-accumulated mutant AR results in marked improvement of SBMA phenotypes (17–19).

Numerous studies have indicated that transcriptional dysregulation is the pivotal mechanism of neuronal dysfunction in polyQ disease. Transcriptional co-activators such as cAMP-response element binding protein-binding protein (CBP) are sequestrated into the NIs through protein–protein interaction in mouse models and patients with polyQ diseases (20,21). Alternatively, the interaction between transcriptional co-activators and soluble mutant protein has also been demonstrated in fly and mouse models as well as in post-mortem tissues of Huntington disease (HD) patients (22,23). The histone acetyltransferase (HAT) activity of CBP is inhibited in a fly model of HD and restored by histone deacetylase (HDAC) inhibitors, resulting in less neurodegeneration (24,25). Oral administration of suberoylanilide hydroxamic acid

*To whom correspondence should be addressed at: Department of Neurology, Nagoya University Graduate School of Medicine, 65 Tsurumai-cho, Showa-ku, Nagoya 466-8550, Japan. Tel: +81 527442385; Fax: +81 527442384; Email: sobueg@med.nagoya-u.ac.jp

(SAHA), an HDAC inhibitor, ameliorates motor impairment in a mouse model of HD (26), but its beneficial effect is restricted by lethal toxicity. In the present study, we report that oral administration of sodium butyrate (SB) ameliorates symptomatic and histopathological phenotypes of a mouse model of SBMA through upregulation of histone acetylation in nervous tissues. Although SB is less toxic than SAHA, this compound yielded beneficial effects within a narrow therapeutic window of dosage. Our results indicate the importance of dose determination in the clinical application of HDAC inhibitors, which are a promising new therapy for polyQ disease.

## RESULTS

### SB improves motor impairment in SBMA mouse model within a narrow optimal dose

SB did not alter the neuromuscular phenotypes in wild-type (Wt) mice at any of the doses we tested (data not shown). Oral administration of SB markedly ameliorated muscle atrophy, body posture and footprint pattern on walking in male Tg mice at a dose of 4 g/l (Fig. 1A and B). We quantitatively assessed motor impairment by rotarod analysis and cage activity measurement, and found remarkable amelioration of motor impairment with oral SB administration in a narrow SB dose range (Figs 2 and 3A–C). SB significantly delayed the onset (at 4 and 8 g/l) and the progression (at 4 g/l) of motor deficit detected by rotarod performance (Figs 2 and 3C). SB also elongated the period during which each motor activity declines to 50% of its maximal value (Fig. 3B). SB did not produce a substantial improvement in such motor performance at 2 g/l (Figs 2 and 3A–C). It should be noted that 16 g/l of SB accelerated the onset by ~2 weeks (Figs 2 and 3C). The number of days for 50% impairment of rotarod and cage activity were not changed with 2 and 8 g/l, but even worsened with 16 g/l (Fig. 3B). Tg mice treated with 16 g/l of SB showed swelling of the kidneys (data not shown), which was also obvious in Wt mice treated with a higher dose, 40 g/l, of SB.

Assessment of survival rate also demonstrated a similar pattern of dose-dependent response to that of motor performance. SB significantly improved the survival rate (4 g/l, $P < 0.0001$; 8 g/l, $P = 0.004$) and time to 50% survival at the dose of 4 and 8 g/l (Figs 2 and 3B), whereas 2 g/l doses of SB did not alter the survival rate (Figs 2 and 3B). On the other hand, the lifespan of Tg mice was shortened at the dose of 16 g/l (Fig. 2, $P = 0.0009$). SB treatment at 4 g/l resulted in body weight gain, whereas Tg mice given other doses of SB showed earlier declines in weight, as did those not treated with SB (Fig. 2).

These observations indicate that oral administration of SB improves motor impairment, survival rate and failure of weight gain in the male Tg mice within a narrow dose range. Nevertheless, a higher dose of SB has deleterious effects on the neurological phenotypes of Tg mice.

### SB ameliorates histopathological impairments of motor neurons and muscles

Oral administration of SB at the dose of 4 g/l significantly improved histopathological impairments in the muscles,

**A**

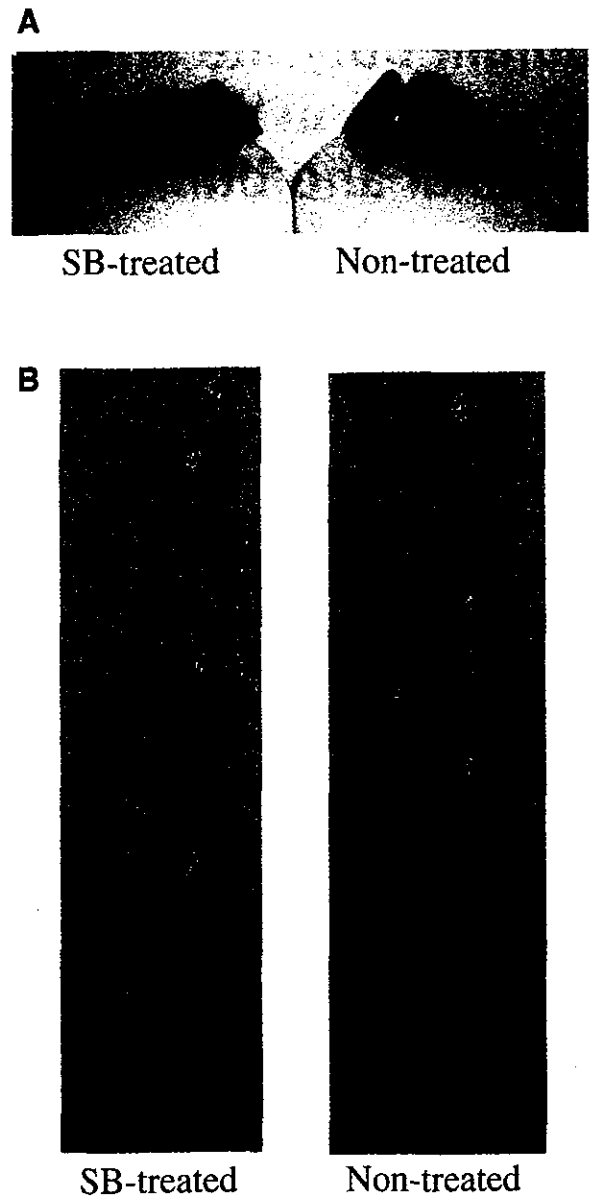SB-treated    Non-treated

**B**

SB-treated    Non-treated

Figure 1. SB ameliorates neuromuscular phenotypes of SBMA Tg mouse. (A) The male Tg mouse treated with 4 g/l of SB does not show the muscular atrophy seen in the non-treated male mouse (12 weeks old). (B) Footprints of the SB-treated and non-treated male Tg mice. Front paws are in red, and hind paws in blue. SB markedly ameliorated gait disturbance.

spinal motor neurons and their axons in the male Tg mice (Fig. 4). The SBMA Tg mice show atrophy of spinal motor neurons and their axons in the ventral nerve root accompanied by neurogenic amyotrophy (17). SB administration significantly increased the diameter of muscles, spinal roots and motor neurons as compared with non-treated mice. Although small angulated fibers and grouped atrophy were observed in the muscles of the non-treated group, SB markedly ameliorated these histopathological appearances of denervation pattern (Fig. 4A–C). SB also improved axonal atrophy in the L5 ventral nerve root (Fig. 4D–F). There was a significant difference in the size of large motor neurons in the lumbar
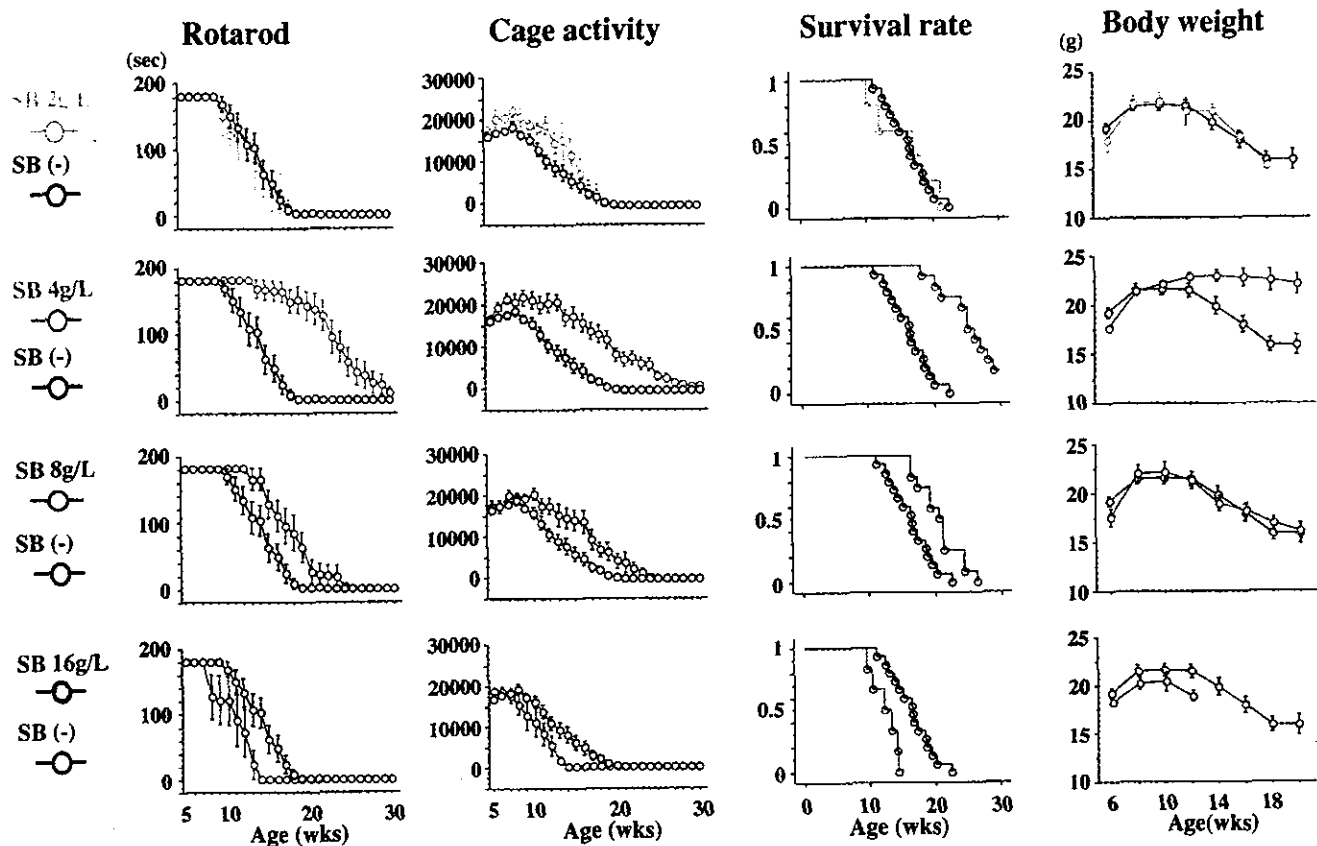
**Figure 2.** SB ameliorates motor abilities of SBMA Tg mice. Rotarod activity, cage activity, body weight and survival rate (Kaplan–Meier) of Tg mice treated with or without SB ($n = 6$ in SB 2 and 16 g/l, $n = 12$ in SB 4 and 8 g/l, $n = 15$ in water).

anterior horn between SB-treated and non-treated male Tg mice (Fig. 4G–I). Quantitative assessment showed a significant improvement in the mean diameter of muscles (45.7 ± 5.7 μm in the SB-treated Tg mice versus 27.2 ± 12 μm in the non-treated Tg mice, $P = 0.005$), the diameter of large axons in the ventral root (>6 μm) (11.2 ± 0.7 μm in the SB Tg mice versus 9.5 ± 0.4 μm in non-treated Tg mice, $P = 0.02$) and the size of large (>300 μm²) motor neurons in the lumbar anterior horn (453.0 ± 32.4 μm² in the SB-treated Tg mice versus 372.0 ± 38.1 μm² in non-treated Tg mice, $P = 0.04$) with oral SB administration at 4 g/l (Fig. 4C, F and I).

### SB does not inhibit nuclear localization and aggregation of mutant androgen receptor protein

As we reported earlier (17), nuclear localization and aggregate formation of the mutant AR protein are the major pathways of neuronal dysfunction and phenotypic expression in SBMA. Thus, we examined whether SB administration alters the amount of nuclear-localized mutant AR and the large complex form of mutant AR protein in male Tg mice, using immunohistochemistry with an anti-polyQ antibody, 1C2 and western blotting analysis. As predicted, SB did not decrease the number of neurons and glial cells harboring diffuse nuclear stain with 1C2 and nuclear inclusions in the spinal cord and other central nervous tissues (Fig. 5A). Similarly,

SB did not change the 1C2 nuclear staining in visceral organs such as muscle (Fig. 5A). The amount of slowly migrating large complex mass and aggregates of the mutant AR in the spinal cords and muscles (Fig. 5B) as well as in their nuclear fractions (Fig. 5C) was assessed by western blotting with an anti-AR antibody, N-20. SB did not alter the amount of smearing mutant AR protein in the stacking gel. Although CBP was sequestered into the nuclear inclusion in Tg mice, oral SB had no influence on CBP distribution (Fig. 5D).

### Oral SB increases histone acetylation level in the central nervous system

It is important to assess the augmentation of histone acetylation in the central nervous system tissue by the oral administration of SB. To determine whether SB increases the acetylation level of histone, we analyzed western blotting of spinal cord homogenate with antibodies against histones H2A, H2B, H3 and H4, and those for acetylated isoforms (Fig. 6A). Without SB treatment, histone acetylation levels are significantly reduced in Tg compared with Wt. Oral SB resulted in a significant increase in the H3 histone acetylation level in male Tg mice at 4 g/l or higher doses, although this effect was not observed at the dose of 2 g/l. The acetylation of histone H3 was also significantly enhanced in Wt mice treated with oral SB (Fig. 6A
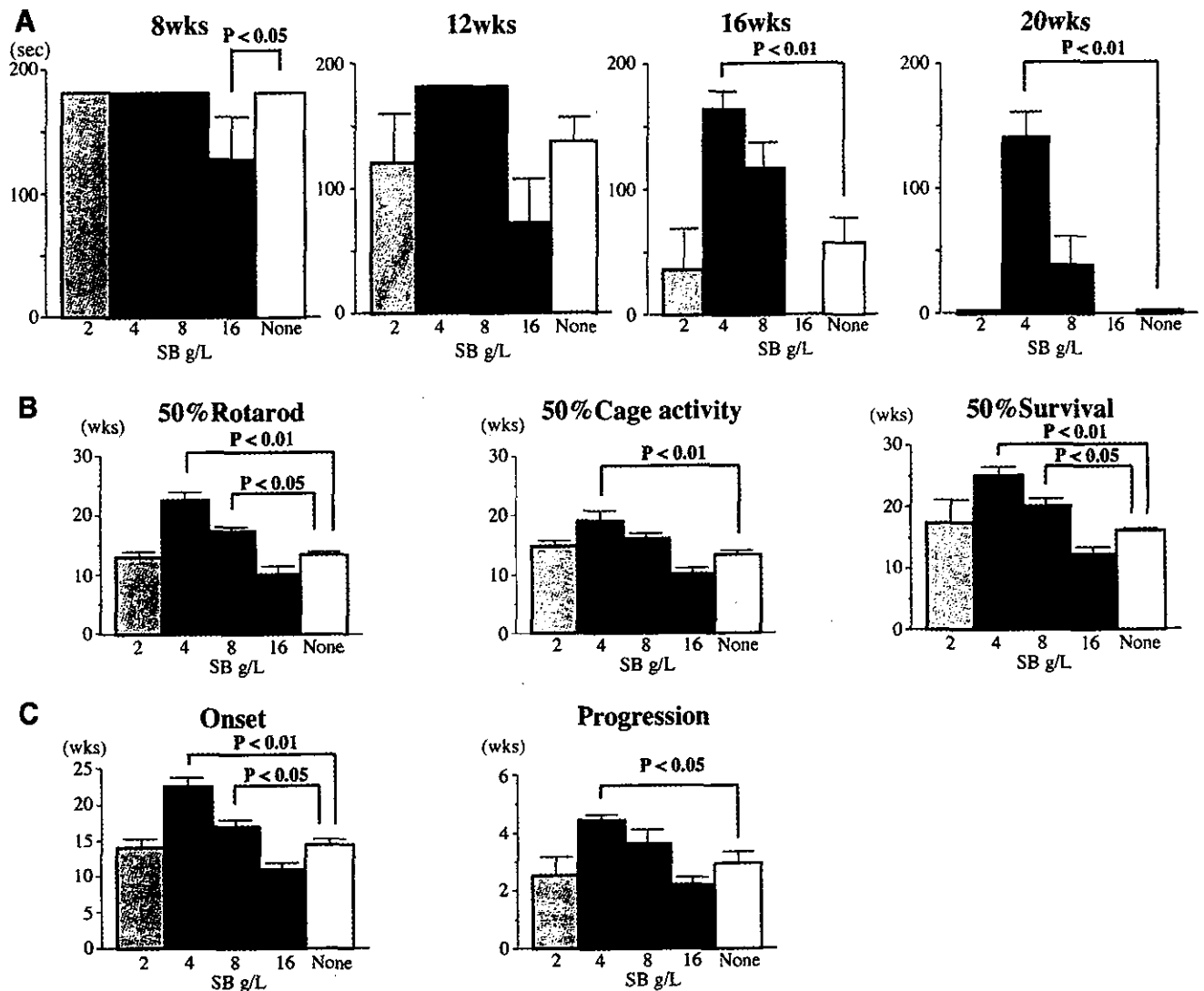
**Figure 3.** SB exerts therapeutic effects within a narrow dose range. (A) Rotarod performance of Tg mice at 8, 12, 16 and 20 weeks of age. The dose effect was bell-shaped at each examined week of age. (B) At the dose of 4 g/l, SB prolonged the period during which motor function, assessed by rotarod task and cage activity, declines to 50% of its maximal value, as well as 50% survival. These effects are also observed at 8 g/l, although to a lesser extent than at 4 g/l. (C) The onset of rotarod task decline and the period from the onset to death in each treatment group. The symptomatic onset is retarded by SB at 4 or 8 g/l, whereas the progression is slowed only at the dose of 4 g/l. (A, B and C: $n = 6$ in SB 2 and 16 g/l, $n = 12$ in SB 4 and 8 g/l, $n = 15$ in water).

and B). In contrast to H3, acetylation of histones H2A, H2B and H4 was not significantly augmented by oral SB administration at any dose (Fig. 6A). Similar effects were observed in the brain and muscle (data not shown).

Immunohistochemistry with the antibody specific to acetyl-ated H3 demonstrated that the nuclei of the spinal cord motor neurons and glial cells were more densely stained in mice given oral SB than in non-treated mice. The staining intensity was proportional to the oral SB doses (Fig. 6C). The numbers of anti-acetylated histone H3 positive neurons and glia cells were significantly greater in SB-treated Tg mice than in non-treated mice (Fig. 6D).

These observations indicate that SB is capable of crossing the blood–brain barrier and increasing the level of H3 acety-lation in the spinal cord and brain, providing the theoretical basis for this SBMA treatment.

## DISCUSSION

A growing number of polyQ diseases share salient clinical features including anticipation and selective distribution of pathology, and their symptoms are influenced by the number of CAG repeats in the causative gene (1,2). Although the gene products are unrelated except for the presence of polyQ tract, some nervous tissues, including the spinal anterior horn, brainstem and cerebellum, are preferentially affected in polyQ diseases. NIs detected in these lesions are the pathological hallmark of the disorders. The observations of common phenotypes led to the hypothesis that unifying mechanisms underlie the pathogenesis of polyQ diseases. Transcriptional dysregulation (16,27,28), aggregate formation (29,30), pro-teolysis of causative protein (31), transglutaminase.activation (32) and mitochondrial deficits (33) have been implicated
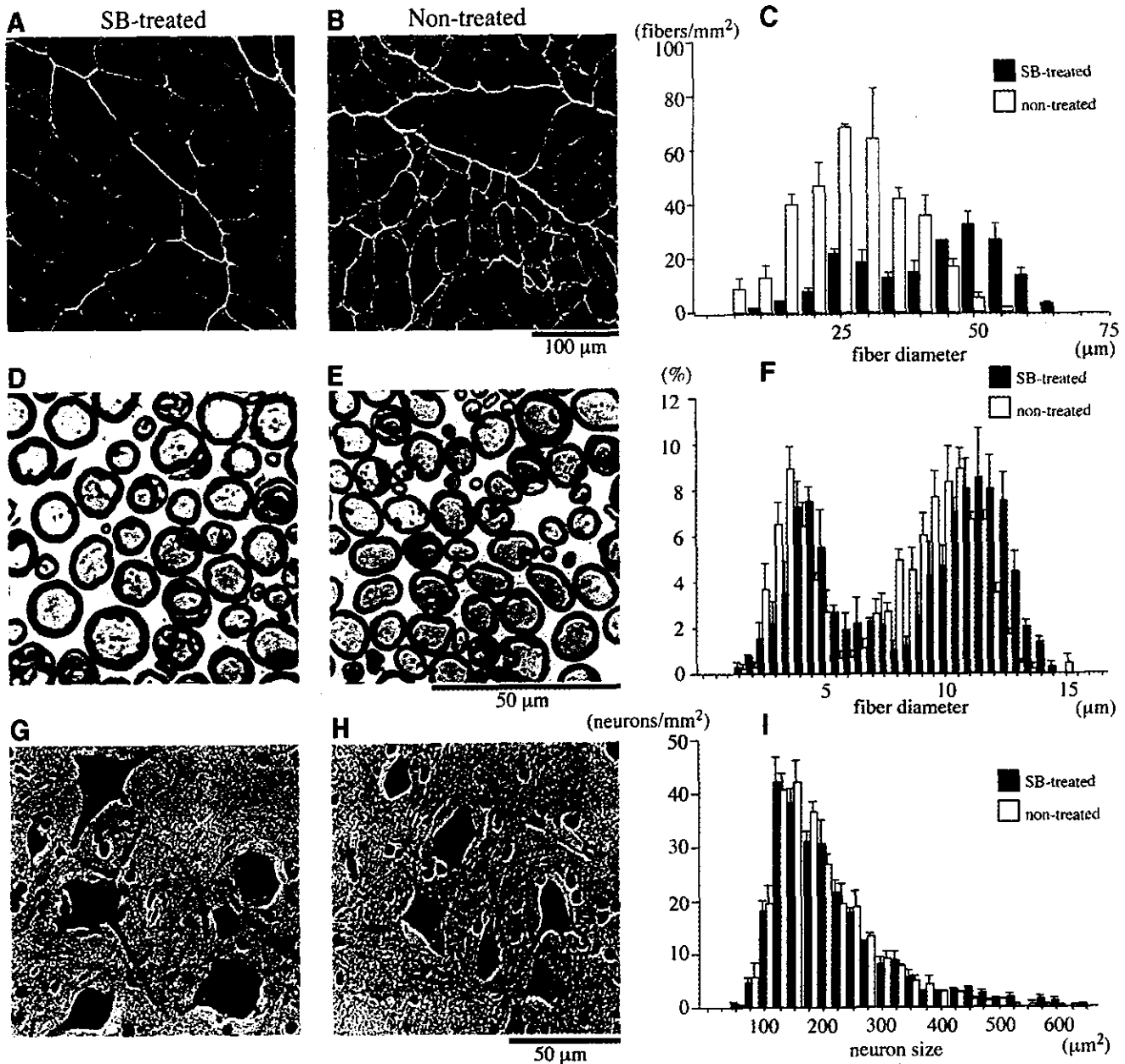
Figure 4. Amelioration of neuropathological findings by SB treatment. (A–C). Muscle H&E staining (A and B) of the SB-treated and non-treated male Tg mice (12 weeks old), and the histogram of muscle fiber diameter (C, $n = 3$ in each group). (D–F) Toluidine blue staining of the L5 ventral root of male Tg mice treated with or without SB (D and E), and the histogram of myelinated fiber diameter (F, $n = 3$). (G–I) Nissl staining of the lumbar anterior horn of Tg mice of each treatment group (G and H), and the histogram of motor neuron size (I, $n = 3$).

in the pathogenesis, and have been expected to be targets of medical intervention. Among these hypotheses, altered transcription appears to be convincing, supported by the fact that most polyQ proteins have been implicated in transcriptional regulation (34).

Gene expression analysis indicates that transcriptional disruption is an early change in the pathogenesis of mouse models of polyQ diseases (35,36). The expression of genes regulated through cAMP-response element-mediated transcription is decreased in HD mouse models (37,38). The transcription co-activators are sequestrated into aggregation,

and their function is inhibited by soluble polyQ-containing protein (2). As the HAT activity of CBP is suppressed in cellular models, a decrease in histone acetylation is likely to underlie the neurodegeneration in polyQ diseases. Although this hypothesis has been confirmed *in vitro*, it remains unclear whether the histone acetylation level is decreased in animal models (26,39). The present study demonstrates that the acetylation of nuclear histone is diminished in SBMA Tg mice, suggesting that the HAT activity of CBP is suppressed *in vivo*. The restoration of histone acetylation by HDAC inhibitors has been considered to be of therapeutic
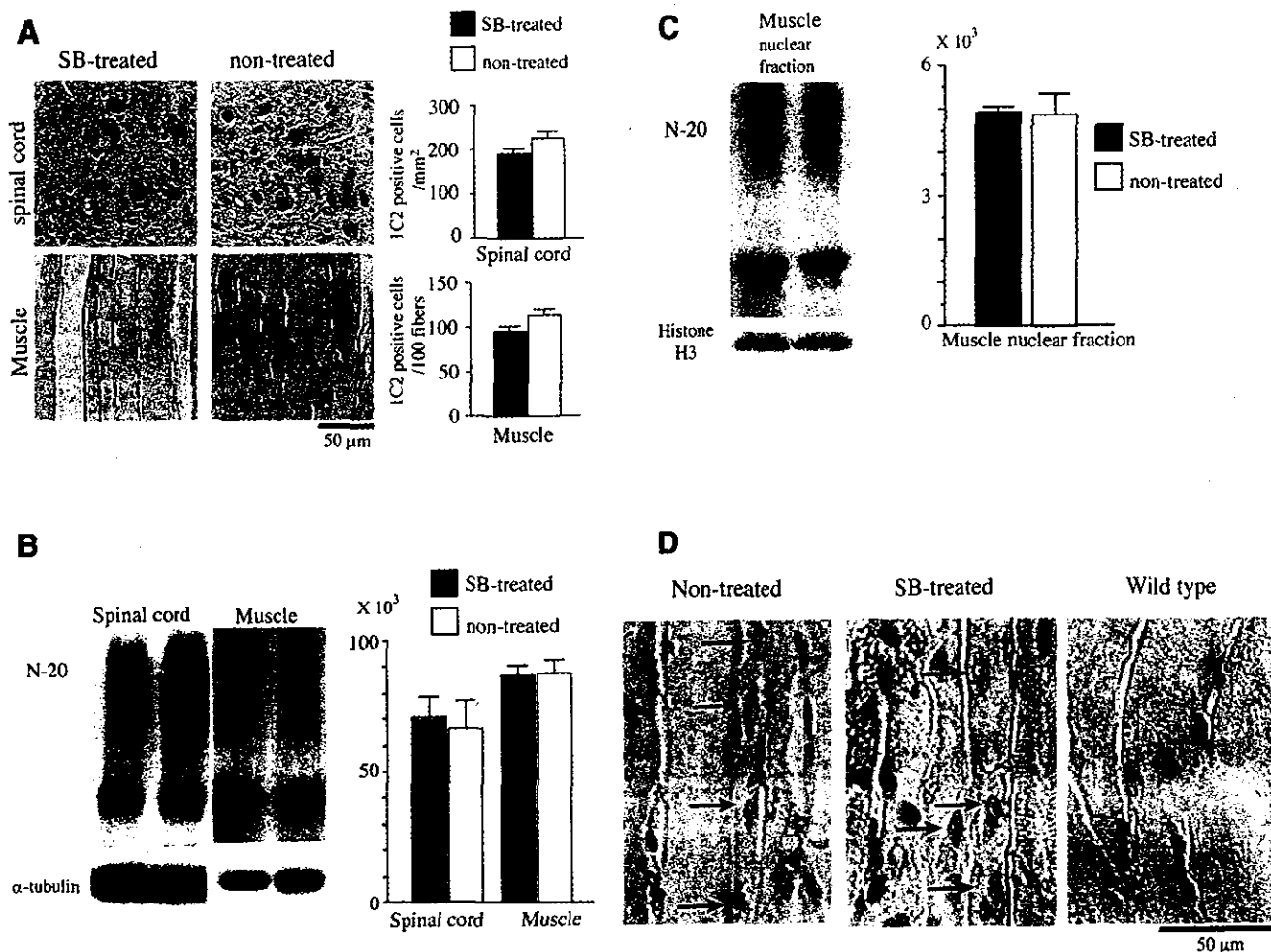
**Figure 5.** SB does not prevent nuclear accumulation of mutant AR. (A) Immunohistochemistry with anti-polyQ antibody of the spinal cord and muscle of Tg mice treated with or without SB (12 weeks old). (B) Western blot analysis with an anti-AR antibody, N-20, of total homogenates from the spinal cord and muscle of the SB-treated and non-treated male Tg mice (12 weeks old). Densitometric analysis demonstrated no difference in the amount of smearing mutant AR protein between SB-treated and non-treated Tg mice ($n = 3$, $P = 0.79$ for spinal cord and $P = 0.93$ for muscle). (C) Western blot analysis of nuclear fraction from the muscle of male mice with N-20 (12 weeks old). In the densitometric analysis, SB did not reduce the amount of smearing mutant AR in the nuclear fraction ($n = 3$, $P = 0.89$). (D) Immunohistochemistry of the muscle demonstrates that CBP is sequestrated into the nuclear inclusion in Tg mice (12 weeks old) regardless of SB treatment.

benefit in polyQ diseases (40). Although HDAC inhibitors mitigate polyQ-induced neurodegeneration in cell and fly models of polyQ diseases (24,25), SAHA is of limited therapeutic benefit in a mouse model of HD owing to its toxicity (26). Based on their ability to regulate transcriptional activity, HDAC inhibitors have also been employed in experimental therapies for malignancies and endocrinological disorders (41). In experimental cancer therapy, as observed in polyQ models, higher doses of HDAC inhibitor are required in animal models than *in vitro*, presumably because of the fast elimination and low bioavailability of these compounds *in vivo*. The cytotoxicity of HDAC inhibitor is considerable, especially in dividing cells, and this needs to be overcome for clinical use. SAHA demonstrated remarkable side effects, including leukopenia, thrombocytopenia, hypotension, acute respiratory distress, renal insufficiency, tumor-related pain and fatigue, in a phase I clinical trial for malignancies (42). Dose-limiting toxicities were neuro-cortical events such as

somnolence and confusion in another phase I clinical trial with phenylbutyrate (43).

SB is less potent than SAHA, but has the advantage of less serious toxicity. Our present study demonstrates that oral SB exerts therapeutic effects with subtle side effects when it is used at an appropriate dose. Our results revealed that the most beneficial effects were achieved at the oral SB dose of 4 g/l, whereas the compound was partially effective at the dose of 8 g/l. The acetylation level of histone is increased at these doses, implying that improvement of transcription contributes to the amelioration of symptomatic and histopathological phenotypes. SB caused no amelioration of the pathogenesis at 2 g/l, presumably because it failed to augment histone acetylation.

It is intriguing that Tg mice had lower tolerance to the toxicity of SB than did Wt. The dose of 16 g/l, which did not harm Wt mice, aggravated motor dysfunction in the Tg mice. This appears to result from the adverse effect of SB,
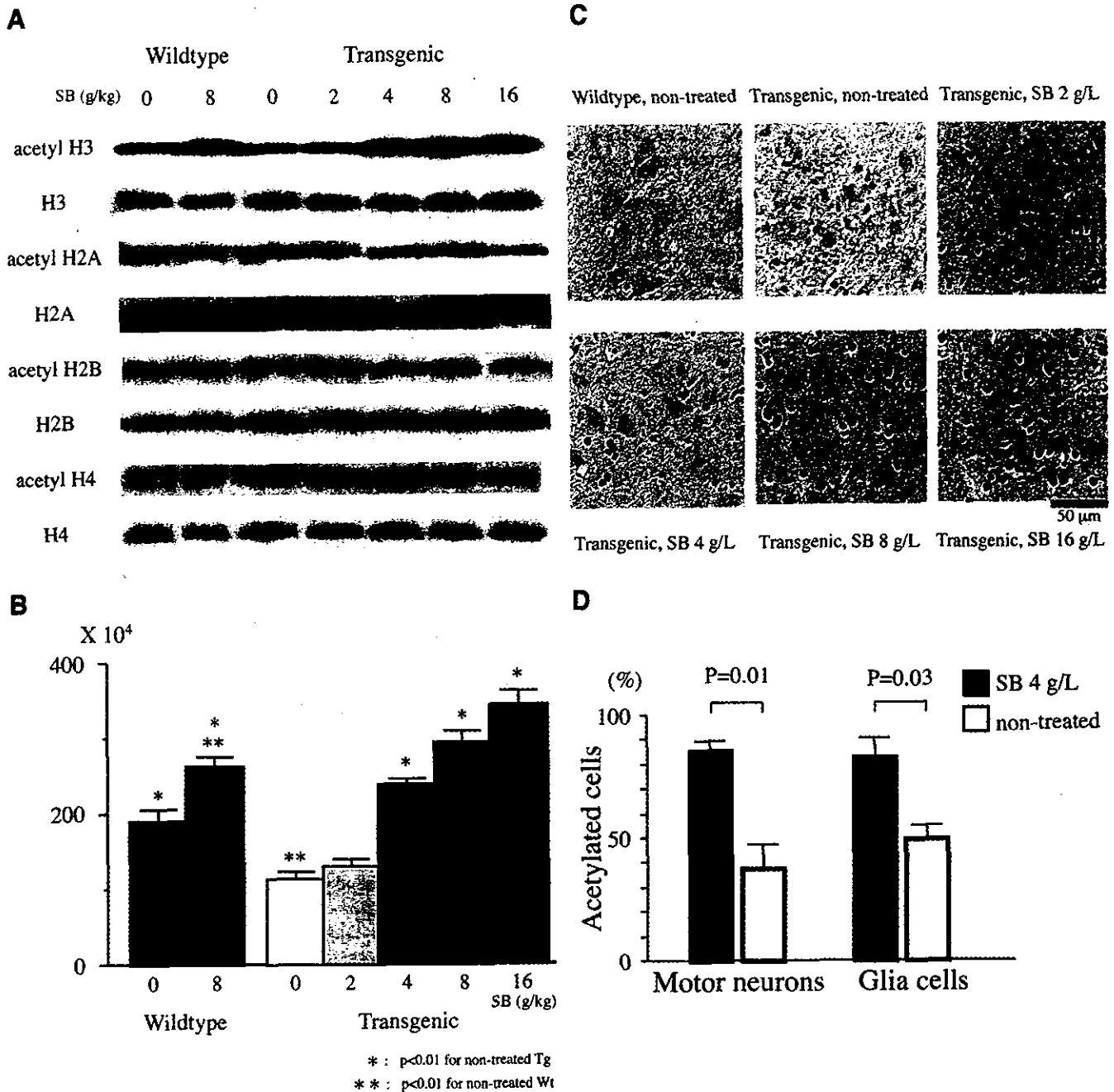
Figure 6. SB induces acetylation of nuclear histone in mice. (A) Western blot analysis of the spinal cord of Wt and Tg mice with the antibodies against histones: H3, H4, H2A and H2B. Each blot was reprobed with the antibodies against the acetylated isoform of the histones. (B) The acetylation level of histone H3 was quantitated using densitometry (n = 6 for each group). (C) Immunohistochemistry of the spinal cord of the SB-treated and non-treated Tg mice with antibodies against acetylated H3. (D) Densitometric analysis of immunohistochemistry shows that the acetylation level of both neurons and glial cells are upregulated at 4 g/l of SB.

as the histone acetylation level was successfully increased in the central nervous system at this dose. SB induces metabolic acidosis and even death at high doses in mice (44). Immobility, dehydration and exhaustion may lower the threshold for adverse effects of SB in Tg mice. This observation should also be kept in mind during clinical trials.

Intraperitoneal delivery of SB has also been reported to ameliorate neurodegeneration in an HD mouse model (39).

This study supports our findings that SB improves the pathogenesis of polyQ diseases at an appropriate dose. Although intraperitoneal administration of SB upregulates acetylation of both histones H3 and H4, the present study demonstrated H3 selectivity of the effect of oral SB treatment. As SB is rapidly eliminated in vivo (44), the route of SB administration may influence its effect on histone acetylation as well as its side effects. Alternatively, a higher dose of SB might be

required for H4 acetylation; indeed, the most effective dose of SB in HD mouse study, 1200 mg/kg/day, was higher than that in our analysis, 800–900 mg/kg/day.

We have previously described therapeutic approaches for SBMA using our Tg mouse model (45). Reduction in the testosterone level by castration or leuprorelin administration diminished nuclear-localized mutant AR and markedly prevented phenotypic expression in the male Tg mice (17,18). Overexpression of heat shock protein 70, which is a molecular chaperone refolding mutant protein (46), resulted in acceleration of mutant AR degradation and phenotypic amelioration (19). Although these strategies show therapeutic promise, single therapeutic agents possess limited potential because of their side effects. As suggested for other neurodegenerative diseases (47), combinations of drugs appear to be useful in the attempts of obtaining maximal therapeutic effects and reducing harmful events. Although the exact mechanism remains to be clarified, SB also ameliorates neuromuscular phenotypes of spinal muscular atrophy, which is another lower motor neuron disease arising from a different gene mutation (48). This result might indicate the relatively potent effects of SB on affected lower motor neurons. SB is a promising candidate for combination therapy for SBMA, although its dose should be very carefully determined for clinical use.

## MATERIALS AND METHODS

### Generation and maintenance of Tg mice and genotyping

Chicken β-actin promoter-driven AR-24Q and AR-97Q constructs were prepared by digestion of pCAGGS vector as described earlier (17,49,50). Genotyping of mice was performed by PCR using mouse tail (17). Tg mice were maintained by crossing to F1 of C57BL/6J and BDF1. We analyzed a symptomatic line #4–6 of this mouse model throughout the present study.

### Assessment of motor ability

All animal experiments were performed in accordance with the National Institute of Health Guide for the Care and Use of Laboratory Animals and were approved by the Nagoya University Animal Experiment Committee. Rotarod performance was assessed weekly using an Economex Rotarod (Colombus Instruments, Colombus, OH, USA) as described previously (51). Cage activity was measured weekly, with each mouse in a transparent acrylic cage within a soundproof box as described previously (17).

### Administration of SB

Wt and SBMA Tg (AR-97Q #4–6) mice were orally supplied sterile water *ad libitum*. Three mice shared the same drinking water in each cage. SB was administered at a concentration of 2, 4, 8, 16 or 40 g/l in distilled water from 5 weeks of age until the end of analysis. Before the onset of motor symptoms, between the age of 6 and 8 weeks, the approximate daily amount of drinking water was similar for each treatment group of Tg mice; 4.0 ± 0.26, 3.7 ± 0.51, 4.5 ± 0.19,

4.1 ± 0.29 and 4.4 ± 0.15 ml at the dose of 0, 2, 4, 8 and 16 g/l, respectively. There was no difference in the amount of water intake and body weight between Wt and Tg mice in that period.

### Immunohistochemistry

An aliquot of 20 ml of 4% paraformaldehyde fixative in 0.1 M phosphate buffer (pH 7.4) was perfused through the left cardiac ventricle of mice (12 weeks old) deeply anesthetized with ketamine–xylazine, the tissues post-fixed in 10% phosphate-buffered formalin and then processed for paraffin embedding. Tissue sections (4 μm thick) were then deparaffinized, dehydrated with alcohol, and then treated for antigen retrieval (17). For the mutant AR immunohistochemical study, the paraffin sections were pretreated with formic acid for 5 min at room temperature. The tissue sections were blocked with normal horse serum (1 : 20) and incubated with mouse anti-expanded polyQ, 1C2 (1 : 10 000, Chemicon, Temecula, CA, USA). The sections were then incubated with biotinylated anti-mouse IgG (1 : 1000, Vector Laboratories, Burlingame, CA, USA). Immune complexes were visualized using streptavidin–horseradish peroxidase (Dako, Glostrup, Denmark) and 3,3′-diaminobenzidine (Dojindo, Kumamoto, Japan) substrate. Sections were counterstained with methyl green. For immunostaining of histone, sections were autoclaved at 121°C for 15 min, and incubated with anti-histone H3 (1 : 100, Upstate Biotechnology, Lake Placid, NY, USA) or anti-acetylated histone H3 (1 : 500, Upstate Biotechnology) antibodies.

The number of 1C2 or anti-acetylated H3-positive cells for one individual mouse was counted using a light microscope with a computer-assisted image analyzer (Luzex FS, Nikon, Tokyo, Japan). Fifty consecutive transverse sections of the thoracic spinal cord were prepared, and 1C2 or anti-acetylated H3-positive cells in the anterior horn on every fifth section were counted as described previously (51,52). For quantitative assessment, 1C2-positive cells in the muscle were calculated from counts of more than 500 fibers in randomly selected areas, and were expressed as the number per 100 muscle fibers.

### Muscle histology and morphometric analysis of spinal motor neurons and ventral spinal roots

Cryostat sections of the gastrocnemius muscles (6 μm thick) were air-dried and stained with hematoxylin and eosin (H&E). The muscle fiber diameter was measured in randomly selected areas for three mice of each treatment group (12 weeks old) using a Luzex FS image analyzer (Nireco). To assess the neuronal populations and cross-sectional area of the anterior horn cells, 20 serial 5 μm thick sections from the fifth lumbar spinal cords of three mice of each group (12 weeks old) were prepared. Every other section was stained by the Nissl technique, and all neurons with an obvious nucleolus in the anterior horn were assessed using a Luzex FS image analyzer as described earlier (17). The diameter of myelinated fibers in the ventral spinal roots was measured on the transverse sections stained with toluidine blue, also as described earlier (17).

## Western blots

Mice (12 weeks old) were exsanguinated under ketamine–xylazine anesthesia, and their tissues snap-frozen with powdered $CO_2$ in acetone. Frozen tissue (0.1 g wet weight) was homogenized in 1000 μl of CelLytic-M mammalian cell lysis/extraction reagent (Sigma Chemical, St Louis, MO, USA) with 1 mM phenylmethylsulfonyl fluoride and aprotinin at 6 μg/ml. Homogenates were spun at 2500g for 15 min at 4°C. The protein concentration of the supernatant was determined using DC protein assay (Bio-Rad Laboratories, Hercules, CA, USA). Each lane on a 5–20% SDS–PAGE gel was loaded with 200 μg protein for the spinal cord and 80 μg for the muscle from the supernatant fraction, which was transferred to Hybond-P membranes (Amersham Pharmacia Biotech, Buckinghamshire, UK) using 25 mM Tris, 192 mM glycine and 10% methanol as transfer buffer. Kaleidoscope prestained standards were used as size markers (Bio-Rad Laboratories). Proteins were then transferred to Hybond-P membranes (Amersham Pharmacia Biotech), which were subsequently blocked in 5% milk in Tris-buffered saline containing 0.05% Tween-20, and incubated with appropriate primary antibodies using standard techniques. Primary antibodies were used at the following concentrations: anti-histone H3, 1:500 (Upstate Biotechnology); anti-acetylated histone H3, 1:250 (Upstate Biotechnology); anti-histone H4, 1:500 (Upstate Biotechnology); anti-acetylated histone H4, 1:200 (Upstate Biotechnology); anti-histone H2A, 1:500 (Upstate Biotechnology); anti-acetylated histone H2A, 1:200 (Upstate Biotechnology); anti-histone H2B, 1:500 (Upstate Biotechnology) and anti-acetylated histone H2B, 1:200 (Serotec, Kidlington, UK). Second antibody probing and detection were performed using the ECL+plus kit (Amersham Pharmacia Biotech) as described earlier (17). The signal intensity of the bands smearing from the top of the gel were quantified using the NIH Image program (NIH Image version 1.62). The quantitative data of three independent western blots were expressed as mean ± SD.

## Statistical analyses

Data were analyzed using Kaplan–Meier and log-rank test for survival rate in Figure 2, Dunnett test for multiple comparison in Figures 3A–C and 6B and unpaired $t$-test in Figures 4, 5 and 6D from Statview software version 5 (HULINKS, Tokyo, Japan).

## ACKNOWLEDGEMENTS

## REFERENCES

1. Zoghbi, H.Y. and Orr, H.T. (2000) Glutamine repeats and neurodegeneration. *Annu. Rev. Neurosci.*, 23, 217–247.
2. Ross, C.A. (2002) Polyglutamine pathogenesis: emergence of unifying mechanisms for Huntington's disease and related disorders. *Neuron*, 35, 819–822.
3. Margolis, R.L. and Ross, C.A. (2002) Expansion explosion: new clues to the pathogenesis of repeat expansion neurodegenerative diseases. *Trends. Mol. Med.*, 7, 479–482.
4. Kennedy, W.R., Alter, M. and Sung, J.H. (1968) Progressive proximal spinal and bulbar muscular atrophy of late onset. A sex-linked recessive trait. *Neurology*, 18, 671–680.
5. Sobue, G., Hashizume, Y., Mukai, E., Hirayama, M., Mitsuma, T. and Takahashi, A. (1989) X-linked recessive bulbospinal neuronopathy. A clinicopathological study. *Brain*, 112, 209–232.
6. Takahashi, A. (2001) Hiroshi Kawahara (1858–1918). *J. Neurol.*, 248, 241–242.
7. La Spada, A.R., Wilson, E.M., Lubahn, D.B., Harding, A.E. and Fischbeck, K.H. (1991) Androgen receptor gene mutations in X-linked spinal and bulbar muscular atrophy. *Nature*, 352, 77–79.
8. Tanaka, F., Doyu, M., Ito, Y., Matsumoto, M., Mitsuma, T., Abe, K., Aoki, M., Itoyama, Y., Fischbeck, K.H. and Sobue, G. (1996) Founder effect in spinal and bulbar muscular atrophy (SBMA). *Hum. Mol. Genet.*, 5, 1253–1257.
9. Tanaka, F., Reeves, M.F., Ito, Y., Matsumoto, M., Li, M., Miwa, S., Inukai, A., Yamamoto, M., Doyu, M., Yoshida, M. *et al.* (1999) Tissue-specific somatic mosaicism in spinal and bulbar muscular atrophy is dependent on CAG-repeat length and androgen receptor–gene expression level. *Am. J. Hum. Genet.*, 65, 966–973.
10. Doyu, M., Sobue, G., Mukai, E., Kachi, T., Yasuda, T., Mitsuma, T. and Takahashi, A. (1992) Severity of X-linked recessive bulbospinal neuronopathy correlates with size of the tandem CAG repeat in androgen receptor gene. *Ann. Neurol.*, 23, 707–710.
11. La Spada, A.R., Roling, D.B., Harding, A.E., Warner, C.L., Spiegel, R., Hausmanowa-Petrusewicz, I., Yee, W.C. and Fischbeck, K.H. (1992) Meiotic stability and genotype-phenotype correlation of the trinucleotide repeat in X-linked spinal and bulbar muscular atrophy. *Nat. Genet.*, 2, 301–304.
12. Igarashi, S., Tanno, Y., Onodera, O., Yamazaki, M., Sato, S., Ishikawa, A., Miyatani, N., Nagashima, M., Ishikawa, Y., Sahashi, K. *et al.* (1992) Strong correlation between the number of CAG repeats in androgen receptor genes and the clinical onset of features of spinal and bulbar muscular atrophy. *Neurology*, 42, 2300–2302.
13. Li, M., Miwa, S., Kobayashi, Y., Merry, D.E., Tanaka, F., Doyu, M., Hashizume, Y., Fischbeck, K.H. and Sobue, G. (1998) Nuclear inclusions of the androgen receptor protein in spinal and bulbar muscular atrophy. *Ann. Neurol.*, 44, 249–254.
14. Li, M., Nakagomi, Y., Kobayashi, Y., Merry, D.E., Tanaka, F., Doyu, M., Mitsuma, T., Fischbeck, K.H. and Sobue, G. (1998) Nonneural nuclear inclusions of androgen receptor protein in spinal and bulbar muscular atrophy. *Am. J. Pathol.*, 153, 695–701.
15. Tobin, A.J. and Signer, E.R. (2000) Huntington's disease: the challenge for cell biologists. *Trends Cell Biol.*, 10, 531–536.
16. Taylor, J.P., Hardy, J. and Fischbeck, K.H. (2002) Toxic proteins in neurodegenerative disease. *Science*, 296, 1991–1995.
17. Katsuno, M., Adachi, H., Kume, A., Li, M., Nakagomi, Y., Niwa, H., Sang, C., Kobayashi, Y., Doyu, M. and Sobue, G. (2002) Testosterone reduction prevents phenotypic expression in a transgenic mouse model of spinal and bulbar muscular atrophy. *Neuron*, 35, 843–854.
18. Katsuno, M., Adachi, H., Doyu, M., Minamiyama, M., Sang, C., Kobayashi, Y., Inukai, A. and Sobue, G. (2003) Leuprorelin rescues polyglutamine-dependent phenotypes in a transgenic mouse model of spinal and bulbar muscular atrophy. *Nat. Med.*, 9, 768–773.
19. Adachi, H., Katsuno, M., Minamiyama, M., Sang, C., Pagoulatos, G., Angelidis, C., Kusakabe, M., Yoshiki, A., Kobayashi, Y., Doyu, M. *et al.* (2003) Heat shock protein 70 chaperone overexpression ameliorates phenotypes of the spinal and bulbar muscular atrophy transgenic mouse model by reducing nuclear-localized mutant androgen receptor protein. *J. Neurosci.*, 23, 2203–2211.
20. McCampbell, A., Taylor, J.P., Taye, A.A., Robitschek, J., Li, M., Walcott, J., Merry, D., Chai, Y., Paulson, H., Sobue, G. *et al.* (2000) CREB-binding protein sequestration by expanded polyglutamine. *Hum. Mol. Genet.*, 9, 2197–2202.
21. Nucifora, F.C. Jr, Sasaki, M., Peters, M.F., Huang, H., Cooper, J.K., Yamada, M., Takahashi, H., Tsuji, S., Troncoso, J., Dawson, V.L. *et al.*

(2001) Interference by huntingtin and atrophin-1 with CBP-mediated transcription leading to cellular toxicity. *Science*, **291**, 2423–2428.

22. Steffan, J.S., Kazantsev, A., Spasic-Boskovic, O., Greenwald, M., Zhu, Y.Z., Gohler, H., Wanker, E.E., Bates, G.P., Housman, D.E. and Thompson, L.M. (2000) The Huntington's disease protein interacts with p53 and CREB-binding protein and represses transcription. *Proc. Natl Acad. Sci. USA*, **97**, 6763–6768.

23. Dunah, A.W., Jeong, H., Griffin, A., Kim, Y.M., Standaert, D.G., Hersch, S.M., Mouradian, M.M., Young, A.B., Tanese, N. and Krainc, D. (2002) Sp1 and TAFII130 transcriptional activity disrupted in early Huntington's disease. *Science*, **296**, 2238–2243.

24. Steffan, J.S., Bodai, L., Pallos, J., Poelman, M., McCampbell, A., Apostol, B.L., Kazantsev, A., Schmidt, E., Zhu, Y.Z., Greenwald, M. *et al.* (2001) Histone deacetylase inhibitors arrest polyglutamine-dependent neurodegeneration in Drosophila. *Nature*, **413**, 739–743.

25. McCampbell, A., Taye, A.A., Whitty, L., Penney, E., Steffan, J.S. and Fischbeck, K.H. (2001) Histone deacetylase inhibitors reduce polyglutamine toxicity. *Proc. Natl Acad. Sci. USA*, **98**, 15179–15184.

26. Hockly, E., Richon, V.M., Woodman, B., Smith, D.L., Zhou, X., Rosa, E., Sathasivam, K., Ghazi-Noori, S., Mahal, A., Lowden, P.A. *et al.* (2003) Suberoylanilide hydroxamic acid, a histone deacetylase inhibitor, ameliorates motor deficits in a mouse model of Huntington's disease. *Proc. Natl Acad. Sci. USA*, **100**, 2041–2046.

27. Cha, J.H. (2000) Transcriptional dysregulation in Huntington's disease. *Trends Neurosci.*, **23**, 387–392.

28. Sugars, K.L. and Rubinsztein, D.C. (2003) Transcriptional abnormalities in Huntington disease. *Trends Genet.*, **19**, 233–238.

29. Bates, G. (2003) Huntingtin aggregation and toxicity in Huntington's disease. *Lancet*, **361**, 1642–1644.

30. Sanchez, I., Mahlke, C. and Yuan, J. (2003) Pivotal role of oligomerization in expanded polyglutamine neurodegenerative disorders. *Nature*, **421**, 373–379.

31. Kobayashi, Y., Miwa, S., Merry, D.E., Kume, A., Mei, L., Doyu, M. and Sobue, G. (1998) Caspase-3 cleaves the expanded androgen receptor protein of spinal and bulbar muscular atrophy in a polyglutamine repeat length-dependent manner. *Biochem. Biophys. Res. Commun.*, **252**, 145–150.

32. Karpuj, M.V., Becher, M.W., Springer, J.E., Chabas, D., Youssef, S., Pedotti, R., Mitchell, D. and Steinman, L. (2002) Prolonged survival and decreased abnormal movements in transgenic model of Huntington disease, with administration of the transglutaminase inhibitor cystamine. *Nat. Med.*, **8**, 143–149.

33. Panov, A.V., Gutekunst, C.A., Leavitt, B.R., Hayden, M.R., Burke, J.R., Strittmatter, W.J. and Greenamyre, J.T. (2002) Early mitochondrial calcium defects in Huntington's disease are a direct effect of polyglutamines. *Nat. Neurosci.*, **5**, 731–736.

34. La Spada, A.R. and Taylor, J.P. (2003) Polyglutamines placed into context. *Neuron*, **38**, 681–684.

35. Lin, X., Antalffy, B., Kang, D., Orr, H.T. and Zoghbi, H.Y. (2000) Polyglutamine expansion down-regulates specific neuronal genes before pathologic changes in SCA1. *Nat. Neurosci.*, **3**, 157–163.

36. Luthi-Carter, R., Strand, A., Peters, N.L., Solano, S.M., Hollingsworth, Z.R., Menon, A.S., Frey, A.S., Spektor, B.S., Penney, E.B., Schilling, G. *et al.* (2000) Decreased expression of striatal signaling genes in a mouse model of Huntington's disease. *Hum. Mol. Genet.*, **9**, 1259–1271.

37. Wyttenbach, A., Swartz, J., Kita, H., Thykjaer, T., Carmichael, J., Bradley, J., Brown, R., Maxwell, M., Schapira, A., Orntoft, T.F. *et al.* (2001) Polyglutamine expansions cause decreased CRE-mediated

transcription and early gene expression changes prior to cell death in an inducible cell model of Huntington's disease. *Hum. Mol. Genet.*, **10**, 1829–1845.

38. Kita, H., Carmichael, J., Swartz, J., Muro, S., Wyttenbach, A., Matsubara, K., Rubinsztein, D.C. and Kato, K. (2002) Modulation of polyglutamine-induced cell death by genes identified by expression profiling. *Hum. Mol. Genet.*, **11**, 2279–2287.

39. Ferrante, R.J., Kubilus, J.K., Lee, J., Ryu, H., Beesen, A., Zucker, B., Smith, K., Kowall, N.W., Ratan, R.R., Luthi-Carter, R. and Hersch, S.M. (2003) Histone deacetylase inhibition by sodium butyrate chemotherapy ameliorates the neurodegenerative phenotype in Huntington's disease mice. *J. Neurosci.*, **23**, 9418–9427.

40. McCampbell, A. and Fischbeck, K.H. (2001) Polyglutamine and CBP: fatal attraction? *Nat. Med.*, **7**, 528–530.

41. Kramer, O.H., Gottlicher, M. and Heinzel, T. (2001) Histone deacetylase as a therapeutic target. *Trends Endocrinol. Metab.*, **12**, 294–300.

42. Kelly, W.K., Richon, V.M., O'Connor, O., Curley, T., MacGregor-Curtelli, B., Tong, W., Klang, M., Schwartz, L., Richardson, S., Rosa, E. *et al.* (2003) Phase I clinical trial of histone deacetylase inhibitor: suberoylanilide hydroxamic acid administered intravenously. *Clin. Cancer Res.*, **9**, 3578–3588.

43. Carducci, M.A., Gilbert, J., Bowling, M.K., Noe, D., Eisenberger, M.A., Sinibaldi, V., Zabelina, Y., Chen, T.L., Grochow, L.B. and Donehower, R.C. (2001) A phase I clinical and pharmacological evaluation of sodium phenylbutyrate on an 120-h infusion schedule. *Clin. Cancer Res.*, **7**, 3047–3055.

44. Egorin, M.J., Yuan, Z.M., Sentz, D.L., Plaisance, K. and Eiseman, J.L. (1999) Plasma pharmacokinetics of butyrate after intravenous administration of sodium butyrate or oral administration of tributyrin or sodium butyrate to mice and rats. *Cancer Chemother. Pharmacol.*, **43**, 445–453.

45. Katsuno, M., Adachi, H., Inukai, A. and Sobue, G. (2003) Transgenic mouse models of spinal and bulbar muscular atrophy (SBMA). *Cytogenet. Genome Res.*, **100**, 243–251.

46. Kobayashi, Y. and Sobue, G. (2001) Protective effect of chaperones on polyglutamine diseases. *Brain Res. Bull.*, **56**, 165–168.

47. Kriz, J., Gowing, G. and Julien, J.P. (2003) Efficient three-drug cocktail for disease induced by mutant superoxide dismutase. *Ann. Neurol.*, **53**, 429–436.

48. Chang, J.G., Hsieh-Li, H.M., Jong, Y.J., Wang, N.M., Tsai, C.H. and Li, H. (2001) Treatment of spinal muscular atrophy by sodium butyrate. *Proc. Natl Acad. Sci. USA*, **98**, 9808–9813.

49. Niwa, H., Yamamura, K. and Miyazaki, J. (1991). Efficient selection for high-expression transfectants with a novel eukaryotic vector. *Gene*, **108**, 193–199.

50. Kobayashi, Y., Kume, A., Li, M., Doyu, M., Hata, M., Ohtsuka, K. and Sobue, G. (2000) Chaperones Hsp70 and Hsp40 suppress aggregate formation and apoptosis in cultured neuronal cells expressing truncated androgen receptor protein with expanded polyglutamine tract. *J. Biol. Chem.*, **275**, 8772–8778.

51. Adachi, H., Kume, A., Li, M., Nakagomi, Y., Niwa, H., Do, J., Sang, C., Kobayashi, Y., Doyu, M. and Sobue, G. (2001) Transgenic mice with an expanded CAG repeat controlled by the human AR promoter show polyglutamine nuclear inclusions and neuronal dysfunction without neuronal cell death. *Hum. Mol. Genet.*, **10**, 1039–1048.

52. Terao, S., Sobue, G., Hashizume, Y., Li, M., Inagaki, T. and Mitsuma, T. (1996). Age-related changes in human spinal ventral horn cells with special reference to the loss of small neurons in the intermediate zone: a quantitative analysis. *Acta Neuropathol.*, **92**, 109–114.

# Previews

## Polyglutamine Diminishes VEGF: Passage to Motor Neuron Death?

Altered gene transcription has been implicated in the pathogenesis of polyglutamine-dependent neurodegeneration. In this issue of Neuron, Sopher et al. demonstrate that androgen receptors containing expanded polyglutamine cause decreased expression of vascular endothelial growth factor (VEGF) by interfering with cAMP response element binding protein binding protein (CBP), thereby contributing to the motor neuron degeneration in spinal and bulbar muscular atrophy.

Expansion of a triplet nucleotide repeat is the molecular basis for a variety of hereditary neuromuscular diseases. At least nine neurodegenerative diseases result from a tedious trinucleotide CAG repeat, which encodes a polyglutamine tract (reviewed in Zoghbi and Orr, 2000). These disorders, called polyglutamine diseases, include spinal and bulbar muscular atrophy (SBMA), Huntington's disease (HD), spinocerebellar ataxias (SCA1, 2, 3, 6, 7, and 17), and dentatorubral pallidoluysian atrophy (DRPLA). Several shared clinical and histopathological features seen in polyglutamine diseases imply a common pathogenesis. The patients suffer from slow progressive neuromuscular symptoms with the onset in adulthood. Although the causative genes are distinct, selected subsets of neurons in the central nervous system undergo degeneration in each disease. Histopathological hallmarks are the loss of neurons in the affected area and the existence of characteristic intranuclear inclusions in the residual neuronal cells. These inclusions contain aggregates of the causative protein together with fundamental cellular components, providing a clue to the mechanisms causing neurodegeneration. Although the precise role of these inclusions remains open to debate, a large body of evidence suggests that the nuclear localization of aberrant polyglutamine protein is an essential step in the pathogenesis.

The perturbation of gene transcription is likely to be among the most substantial nuclear events in the pathophysiology of polyglutamine diseases. This hypothesis emerged from the observation that cAMP response element binding protein binding protein (CBP), a transcriptional coactivator, is sequestrated into the polyglutamine inclusion (Nucifora et al., 2001). Furthermore, the acetyltransferase activity of CBP is directly inhibited by the interaction with aberrant polyglutamine protein (Steffan et al., 2001). In agreement with these findings, alteration of a wide range of gene expression has been detected in mouse models of polyglutamine diseases (Sugars and Rubinsztein, 2003). It is of therapeutic significance that polyglutamine-mediated neurodegeneration in a Drosophila model of HD is alleviated by histone

deacetylase inhibitors, which restore histone acetylation and upregulate gene transcriptions (Steffan et al., 2001). Although decreased transcription appears to be a plausible explanation for the pathogenesis, little direct link between CBP dysfunction and neurodegeneration has been clarified in vivo. In addition, it remains unclear which gene is responsible for neuronal cell death in each polyglutamine disease.

Spinal and bulbar muscular atrophy (SBMA), or Kennedy's disease, which is caused by an expanded CAG repeat in the androgen receptor (AR) gene, was the first disease to be identified as a polyglutamine disease (La Spada et al., 1991). SBMA is an adult-onset lower motor neuron disease characterized by proximal muscle atrophy, weakness, fasciculations, and bulbar involvement. In the central nervous system, the brainstem and the anterior horn are selectively involved. Besides motor neuron degeneration, patients present with several systemic complications: gynecomastia, hyperlipidemia, and glucose intolerance. Since the loss of AR function does not result in neuromuscular phenotypes, the extended polyglutamine tract itself appears to render the causative protein toxic, as documented in other polyglutamine diseases. The disruption of CBP-mediated transcription has also been implicated in the pathogenesis of this disease (McCampbell et al., 2001). Despite a common molecular basis, SBMA is distinct from other polyglutamine diseases in that males are exclusively affected. A transgenic mouse model of SBMA revealed that ligand-dependent nuclear translocation of the pathogenic AR protein accounts for the gender-related pathogenesis, leading to the development of a potential hormonal therapy for this disorder (Katsuno et al., 2002).

In this issue of Neuron, Sopher et al. (2004) report a new transgenic mouse model carrying human AR yeast artificial chromosome (YAC) with a prolonged CAG repeat. Their study reconfirmed the importance of nuclear accumulation of aberrant AR and ligand-dependent pathophysiology in SBMA. Since the expression of the transgene is controlled by its own promoter, the mRNA level of the mutant AR in this model is less than that in previous mouse models using potent exogenous promoters. This would account for the pathological distribution reminiscent of SBMA and the slow progression of motor disability. Among the conspicuous achievements in this study is the finding that the transgenic mice recapitulate the loss of lower motor neurons in SBMA. Whereas histopathological studies of autopsy cases with polyglutamine diseases show a tangible loss of neurons in lesions, a majority of transgenic mouse models demonstrate neuromuscular disability without detectable cell death (Zoghbi and Orr, 2000). This could be explained by the short life span and excessive expression of the causative polyglutamine protein in these mouse models. Symptomatic phenotypes with normal cell populations may indicate that the pathophysiology of polyglutamine disease rises from the dysfunction of neurons. This hypothesis in turn indicates the reversibility of the pathogenesis at the early stage of the diseases. In support of this view, the interruption of mutant gene
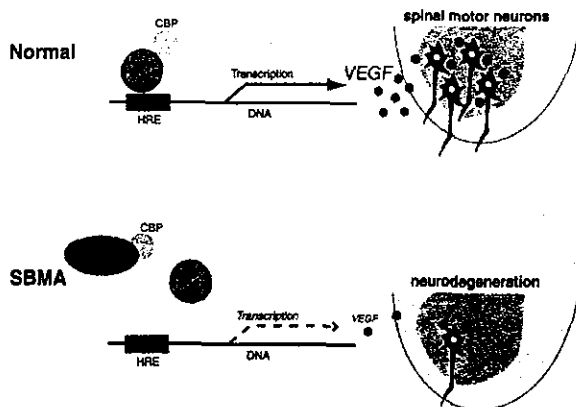
Figure 1. Possible Mechanism of VEGF-Related Motor Neuron Degeneration in SBMA

Hypoxia-inducible factor $1\alpha$ (HIF-$1\alpha$) binds to hypoxia-response element (HRE) in the promoter of vascular endothelial growth factor (VEGF), upregulating its transcription. This transactivating activity of HIF-$1\alpha$ is facilitated through interaction with cAMP response element binding protein binding protein (CBP). In spinal and bulbar muscular atrophy (SBMA), the pathogenic androgen receptor (AR) containing expanded polyglutamine (polyQ) interacts with CBP, resulting in decreased level of VEGF. These processes appear to contribute to motor neuron degeneration in SBMA.

expression reversed the symptoms and histopathological features in a conditional mouse model of HD using a tet-regulation system (Yamamoto et al., 2000). Although this observation justifies medical intervention to mildly affected or presymptomatic patients, elucidating the precise mechanism giving rise to neuronal cell death is also essential for the development of therapies for polyglutamine diseases. The study of Sopher et al. appears to offer a striking insight into the pathophysiology of polyglutamine-induced motor neuron death, in their revelation that the interaction between pathogenic AR and CBP results in a reduced expression of vascular endothelial growth factor (VEGF), which appears to contribute to the neurodegeneration in SBMA.

VEGF, first discovered as a factor enhancing vascular permeability, plays a crucial role in physiological and pathological angiogenesis. Diverse biological effects of VEGF are facilitated by its receptor, VEGF-2, also termed kinase insert domain receptor (KDR). The gene expression of VEGF is drastically upregulated upon hypoxia in order to form new blood vessels. Hypoxia-inducible factors, HIF-$1\alpha$ and HIF-$2\alpha$, mediate this cellular protective response through binding to hypoxia-response element (HRE) in the promoter of VEGF. The transactivating activity of HIF-$1\alpha$ is facilitated through interaction with transcriptional coactivators such as CBP (Figure 1). The depletion of a single allele of VEGF results in embryonic lethality, whereas lack of the HRE sequence in the VEGF promoter leads to slowly progressive motor neuron degeneration (Oosthuyse et al., 2001). Knockin mice harboring a VEGF gene in which HRE is deleted demonstrate a late-onset motor neuron disease resembling SBMA and amyotrophic lateral sclerosis (ALS), suggesting a pivotal role for VEGF in neurodegeneration. The low expression level of VEGF in these mice results in loss of spinal motor neurons, axonal degeneration in

the peripheral nerve, and neurogenic muscular atrophy, all of which are pathological features of human motor neuron diseases. Moreover, the targeted disruption of HRE results in the marked exacerbation of motor neuron degeneration in transgenic mice carrying mutant superoxide dismutase 1 (SOD 1), the most frequent cause of familial ALS (Lambrechts et al., 2003). The deleterious effects of HRE deletion on motor neurons could be due to the suppression of favorable effects of VEGF: enhancement of blood supply and direct neuroprotection. Given that intraperitoneal administration of VEGF ameliorates ischemia-induced degeneration of spinal motor neurons in the aberrant VEGF knockin mice (Lambrechts et al., 2003), blood circulation insufficiency may cause neuromuscular phenotypes. Since VEGF protects cultured normal motor neurons from apoptotic stimuli, loss of these neurotrophic effects could also contribute to the pathogenesis of motor neuron degeneration due to HRE deletion.

The study of Sopher et al. shows that the reduction in the expression level of VEGF precedes the onset of neurogenic muscular atrophy, suggesting that the transcriptional alteration is a trigger, rather than a consequence, of neurodegeneration. The implication of VEGF in SBMA is also backed by the observation that an exogenous VEGF administration alleviates cytotoxicity induced by pathogenic AR with expanded polyglutamine in their cell model. In addition, CBP cotransfection augments VEGF level in the same cultured motor neurons, implying that the transactivating ability of CBP is suppressed by an aberrant protein-protein interaction with AR. This work sheds light on VEGF as a key player in the pathogenesis of polyglutamine-induced motor neuron degeneration, providing another therapeutic target for SBMA. The retrograde delivery of neurotrophic factors ameliorates neurodegeneration in mouse models of motor neuron diseases to some extent (Kaspar et al., 2003). It should be of value to investigate whether VEGF administration improves the polyglutamine-dependent pathogenesis in the SMBA mouse model of Sopher et al. Alternatively, the repressed transcription of VEGF in SBMA mice suggests that chronic hypoxia aggravates motor neuron degeneration, although its clinical implications have yet to be elucidated. Chronic ischemia, aggravated by lowered level of VEGF, appears to induce oxidative stress, which has been suggested to exacerbate neurodegenerative processes. It thus seems possible that polyglutamine-induced pathophysiology could be ameliorated by antioxidative therapy, which should be tested elsewhere.

A great deal of effort has been made to clarify the exact mechanism causing neuronal dysfunction and the process leading to cell death in polyglutamine diseases. Multiple pathophysiological steps may plunge neurons from dysfunction to death in the presence of an expanded polyglutamine tract. The transcriptional dysregulation of VEGF is likely to play an important role in polyglutamine-induced motor neuron death, since the HRE-deleted mice also showed loss of spinal motor neurons (Oosthuyse et al., 2001). However, whether this hypothesis accounts for the whole pathogenesis of SBMA remains to be resolved. Given that multiple mechanisms are involved in neurodegeneration, we need to clarify which genes, regulated by CBP or other factors,